

**NASA Contractor Report 181693**

**ICASE REPORT NO. 88-44**

# ICASE

RECENT INSIGHTS INTO INSTABILITY AND TRANSITION  
TO TURBULENCE IN OPEN-FLOW SYSTEMS

Mark V. Morkovin

(NASA-CR-181693) RECENT INSIGHTS INTO  
INSTABILITY AND TRANSITION TO TURBULENCE IN  
OPEN-FLOW SYSTEMS Final Report (NASA) 84 p  
CSCI 20D

N88-30079

Unclas  
G3/34 0161712

Contract Nos. NAS1-18107 and NAS1-18605  
August 1988

**INSTITUTE FOR COMPUTER APPLICATIONS IN SCIENCE AND ENGINEERING**  
NASA Langley Research Center, Hampton, Virginia 23665

Operated by the Universities Space Research Association



National Aeronautics and  
Space Administration

Langley Research Center  
Hampton, Virginia 23665

RECENT INSIGHTS INTO INSTABILITY AND TRANSITION  
TO TURBULENCE IN OPEN-FLOW SYSTEMS

Mark V. Morkovin  
Department of Mechanical and Aerospace Engineering  
Illinois Institute of Technology, Chicago, IL 60616  
Consultant to ICASE, Hampton, VA. 23665

Abstract

Roads to turbulence in open-flow shear layers are interpreted as sequences of often competing instabilities. These correspond to primary and higher-order restructurings of vorticity distributions which culminate in convected spatial disorder (with some spatial coherence on the scale of the shear layer) traditionally called turbulence. Attempts are made to interpret these phenomena in terms of concepts of convective and global instabilities on one hand, and of chaos and strange attractors on the other. The first is fruitful, and together with a review of mechanisms of receptivity provides a unifying approach to understanding and estimating transition to turbulence. In contrast, current evidence indicates that concepts of chaos are unlikely to help in predicting transition in open-flow systems. Furthermore, a distinction should apparently be made between temporal chaos and the convected spatial disorder of turbulence past Reynolds numbers where boundary layers and separated shear layers are formed.

---

This research was supported by the National Aeronautics and Space Administration under NASA Contract Nos. NAS1-18107 and NAS1-18605 while the author was in residence at the Institute for Computer Applications in Science and Engineering (ICASE), NASA Langley Research Center, Hampton, VA 23665.

AIAA - 88 - 3675

RECENT INSIGHTS INTO INSTABILITY AND TRANSITION  
TO TURBULENCE IN OPEN-FLOW SYSTEMS

Mark V. Morkovin  
Department of Mechanical and Aerospace Engineering  
Illinois Institute of Technology, Chicago, IL 60616  
Consultant to ICASE, Hampton, VA. 23665

1. INTRODUCTION

Information on instabilities and transition to turbulence in shear layers has amplified exponentially in recent years and useful earlier summaries Morkovin (1978), Reshotko (1976, 1984), Arnal (1984), Ho and Huerre (1984), Schlichting (1979) and others can serve only as essential points of departure for a novice in the field.

This report represents a selective account of the more recent insights into transition mechanisms in open-flow systems, Fig. 1, as well as some new questions and disagreements that have arisen and that

may challenge innovative researchers. This up-to-date perspective is presented by focusing on vorticity fields: the transition process consists of a sequence of often competing instabilities which correspond to primary and higher-order restructuring of vorticity distributions. Use of composite figures was chosen as a key tool to convey and summarize overall features and contrasting developments. A careful student of the subject will supplement these views with others, especially more mathematical approaches such as that of Bayly, Orszag and Herbert (1988). Spatial constraints limited the number of references; mostly they were chosen as particularly illustrative and suggestive. From these references and discussions in them a broader bibliography can be readily compiled.

Two recurrent themes wind their way through the text: (1) response of shear layers to external stimulation, "natural" (indigenous to their specific environments) and intentional, by vibrations, sound, protuberances, grids, etc. for controlled modifications of behavior, and (2) comparison of instability and turbulence behavior in open-flow and closed-flow systems. The first theme rests on the recent clarification of concepts of convective and global instability and proves itself very fruitful. It is coupled with the mechanisms of receptivity by which the external disturbances get internalized as unstable intrinsic shear-layer vorticity modes. The second theme aims at the possible applicability of the concepts of chaos and strange attractors to the open-flow systems. A simple introduction to these concepts is given in the Appendix with emphasis on the first theme: response to harmonic forcing.

Broadly speaking, open-flow systems, Fig. 1, have two distinguishing behavior patterns not seen in the inherent oscillatory motions of non-fluid systems: downstream propagating primary instabilities within a broad band of frequencies, and (at the end of a sequence of higher-order instabilities) spatially disorderly turbulence with some spatial coherence on the scale of the shear layer (the coherent "large scale" structures). All convectively unstable open flows at higher Reynolds numbers display their particular disturbance-conditioned sequence of instabilities successively in  $x$  (the streamwise coordinate) at the same time  $t$ . Restructuring of

vorticity probably continues in all shear layers with x-varying thickness. Only far downstream in internal flows, Fig. 1b, can a true equilibrium of turbulence possibly take place.

In contrast, within closed-flow systems the flow interacts with itself at all times. Under this iterative self-interaction, equilibrium states at constant Reynolds number (including turbulent states) are generally reached in a short time at all spatial locations. A fixed Reynolds or Rayleigh number and a fixed stable oscillatory equilibrium can usually be set at will and maintained in time by the experimenter-designer. It will be seen that these differences impair the applicability of the concepts of chaos to open-flow systems.

The interweaving of the two themes and the structure of the paper can be gleaned from the Table of Contents and the sequence of figures.

#### TABLE OF CONTENTS

##### Abstract

1. Introduction
2. Roads to turbulence in open-flow systems
  - 2.1 Dehomogenizing, linearized primary instabilities
  - 2.2 Amplification and damping of first and higher normal modes
  - 2.3 Nonlinear developments: secondary and higher instabilities
  - 2.4 Parametric instabilities
  - 2.5 When does a turbulent state set in? What is it?
  - 2.6  $Re_{mint}$ ,  $Re_{cr}$ ,  $Re_{tr}$  and bypass transition
  - 2.7 Relaminarization
3. Convective instability and streamwise resonance
  - 3.1 Local convective and absolute instability
  - 3.2 Linear resonance in x, nonlinear effects and pressure feedback
  - 3.3 Noise response in convectively unstable layers
  - 3.4 Absolute versus global instability

- 3.5 Convective-hydroacoustic global instability, numerical simulations
- 4. Nature and role of receptivity
  - 4.1 Receptivity-conditioned weak global instability in mixing layers
  - 4.2 Noise amplification in mixing layers
  - 4.3 Illustration of unsteady forcing of boundary layers
  - 4.4 On forcing of shear layers by quasisteady fields; Goertler instability
  - 4.5 Environmental forcing in open flow systems
  - 4.6 Receptivities to unsteady pressure fields
  - 4.7 Unknown receptivity paths
- 5. Chaos and turbulence in open-flow shear layers
  - 5.1 Instabilities, forcing disturbances, receptivities and chaos predictions
  - 5.2 The case of a chaotic laminar slender wake
  - 5.3 Road to turbulence in a globally unstable flow
  - 5.4 Road to turbulence in a boundary layer;  $e^N$  method
  - 5.5 On experiments on chaos in open-flow systems
- 6. Conclusions
- A Appendix: A taste of chaotic behavior
  - A-1 New concepts and philosophical implications
  - A-2 Limit cycle-attractor
  - A-3 Oscillator forcing - three dimensional phase space
  - A-4 On implications for open-flow systems
- R References
- F Figures

## 2. ROADS TO TURBULENCE IN OPEN-FLOW SYSTEMS

(2.1) Dehomogenizing, linearized primary instabilities.

Instabilities arise primarily in thin shear layers generated by viscosity in flows past solid walls: boundary layers, wakes, jets, mixing layers, pipe and duct flows, etc. At lower Reynolds numbers,  $Re$ , the laminar velocity profiles (such as those in Fig. 2 for mixing layers, flat and concave boundary layers) form quasi-two-dimensional continuous vorticity distributions which are nearly homogeneous in the streamwise  $x$  and spanwise  $z$  directions. As  $Re$  increases, vorticity dynamics lead to locally increased concentrations  $\Delta\omega$  associated with the first or primary instability as sketched in mid Fig. 2. This first restructuring of vorticity consists thus of dehomogenization or lumpization of the  $\omega$  field in which total vorticity is preserved.

In the case of the concave boundary layer, incremental positive and negative streamwise vortices, named after Goertler and Taylor, grow in  $x$ , Fig. 2 right, while the flow remains steady. In the case of the flat-plate boundary layer, positive and negative intensifications of spanwise vorticity  $\Delta\omega$  are convected downstream at speed  $c$ . The dehomogenization together with convection render the flow unsteady. However, an observer traveling downstream with speed  $c$  would see a steady growth of the concentration in the so-called Kelvin cat's eyes, located slightly above the critical height  $y_{cr}$  (for which  $U(y_{cr}) = c$ ), center of Fig. 2. In the case of the antisymmetric mixing layer on the left of Fig. 2 spanwise  $\Delta\omega$  grow in time and remain in place.

(2.2) Amplification and damping of first and higher normal modes

This restructuring in open-flow systems generally proceeds from vorticity disturbances (nonhomogeneous in space and/or time) induced by small perturbations in the environment of the given shear layer. The initial growth rate of the vorticity concentrations can be computed from the linearized Navier-Stokes equations for the local geometry of the layer. When excitation is purely sinusoidal, the response consists

of a superposition of normal or eigen modes associated with the local, nearly parallel structure of the shear layer. In general, all but the lowest mode are damped. Above a geometry-dependent minimum critical Reynolds number,  $Re_{cr}$ , the lowest mode is selectively amplified in relatively narrow frequency and/or wave number band. The corresponding y-distribution of vorticity, velocity components, pressure, etc are called eigen or characteristic functions and can at times be verified experimentally. They grow proportionately to the cosine-exponential combinations shown under the sketches in Fig.2. Thus, the incremental vortices in the mixing layer case intensify in place at the temporal exponential rate  $\alpha_r c_i$  per unit time (where wave number  $\alpha_r$  is the inverse of the wavelength  $\lambda$  multiplied by  $2\pi$  and  $c_r, c_i$  are the real and imaginary components of the complex "propagation speed "c). For the other two cases in Fig.2, the exponential amplification rate is spatial in character,  $-\alpha_i$  per unit length, where  $\alpha_r, \alpha_i$  are the real and imaginary parts of the complex wave number  $\alpha$ , again computed as eigenvalues for the given system of linear equations.

### (2.3) Nonlinear developments: secondary and higher instabilities

It has been recently established that nonlinear effects, neglected in the above computations, can initiate secondary resonance mechanisms when the r.m.s. x - velocity fluctuations  $u'$  reaches relatively low levels of 0.3 percent of the mean velocity  $U_e$  at the edge of a flat-plate boundary layer. In mixing layers secondary restructuring commonly begins at primary  $u'$  levels near  $0.001 \cdot U_e$ , while the primary vortex growth and roll-up continues nearly exponentially to saturation levels on the order of  $0.1 \cdot U_e$ . (The cited  $u'$  levels convey relative not absolute energetics. In experiments, even numerical ones, the energies are contained in nonstandardized finite band-widths, which vary among experimenters.) It is important to note that slower, hardly diagnosable three-dimensional tertiary restructuring may commence almost hand in hand, with the secondary vortex-pairing instability.

These observed cases thus do not conform to the scenario postulated by most mathematicians, namely that the primary instability should first reach a nonlinear equilibrium. Such a "saturated" equilibrium



flow would form a new base flow which, in principle, could be perturbed and linearized in order to characterize the secondary instability modes bifurcating from the equilibrium flow. One reason for the growth of secondary instabilities from non-equilibrium states is the fact that these shear layers constantly grow in thickness. That thickness is taken as constant in the bifurcation theory. Another reason may be that in the strictly parallel boundary layer case the bifurcation is "subcritical". Subcriticality implies that the finite-amplitude equilibrium, if achievable, would be automatically unstable. Herbert (1988) describes in great detail the experimental and theoretical research which resulted in the current understanding of secondary instabilities in boundary layers (summarized in the center of our Fig 15.) Even though the instabilities start from non-equilibrated new base flows, the assumption of a saturated primary leads to a very satisfactory agreement with experiments, Herbert (1988).

#### (2.4) Parametric instabilities

Herbert also stresses that all the first restructurings bring about systems of equations in which some coefficients of the unknowns vary periodically in space or time, say with period  $P$ , as sketched in Fig. 2. The resulting linear Floquet equations exhibits powerful parametric instabilities, with periods  $(m/n) P$ , where  $m$  and  $n$  are integers. Thus there are many possible competing secondary instabilities, depending on initial conditions and on the "saturated" amplitude of the primary mode (threshold effects). Consequently, for each physical realization, such as those in Fig. 2, this unified mathematics will be reflected in different competing geometrical vorticity formations. In mixing layers, the especially strong subharmonic instability with  $m = 2$  and  $n = 1$ , may correspond to pairing of two-dimensional primary vortices with total vorticity conserved or to a three-dimensional corrugation of the primary vortices, with the quintessential new-vorticity generating mechanism by "tilting and stretching"; see theory of Pierrehumbert and Widnall (1982) and experiments described by Ho and Huerre (1984). For the flat plate boundary layer in Fig. 2, the three-dimensional secondary instability ( $m = 2$ ,  $n = 1$ ) is present in the Craik (small amplitude) and Herbert (finite amplitude) mechanisms. The earlier explored secondary instability, the K

mechanism, studied experimentally by Klebanoff, Tidstrom and Sargent (1962), corresponds to  $m = 1$  and  $n = 1$ , and to a higher threshold amplitude of the primary instability.

(2.5) When does a turbulent state set in? What is it?

As indicated in the summary Fig. 3, higher instabilities, i.e., rapid restructurings of vorticity are observed as  $Re$  increases, often simultaneously on different scales. In closed flow systems, such as flows between rotating cylinders, the successive instabilities are relatively clear cut. Yet there is competition between the many possible configurations. Also, localized regions of turbulence occur, especially in counter-rotation, see Andereck, Liu and Swinney (1986). In open-flow systems with shear layer thickening in  $x$  or  $t$ , lack of resolving power of our instruments limits identification of instabilities beyond the tertiary, - if any are present. In a short time or distance past the occurrence of the tertiary we are generally unable to distinguish the state of the flow from a classically turbulent one. According to Tennekes and Lumley (1987) and R. W. Stewart (1968) four key syndromes characterize turbulence encountered in engineering, Fig. 3,: (1) irregularity, (2) three-dimensional vorticity, (3) diffusive motions far in excess of molecular mixing, and (4) dissipation. The first three are useful in diagnostics: they imply broad band (three dimensional) spectra. In motion-picture visualizations the onset of turbulence at higher Reynolds numbers is commonly seen as a sporadic sudden localized increase in diffusion which obliterates small regions of laminar streak lines as an "incipient turbulent 3D spot" is formed in the final stage of instability.

Such emerging turbulent 3D spots need to be distinguished clearly from the turbulent spots and patches studied experimentally in boundary layers and ducts which are often called Emmons' spots. Emmons' spots grow in an environment of nearly quiescent laminar layer whereas the neighborhood of the incipient turbulent 3D spots, though still laminar, is highly unsteady and contains significant three-dimensional vorticity. Dynamics of their subsequent growth are unlikely to be comparable.

To what extent are the classically turbulent states in open-flow systems (as characterized by the above four syndromes) equivalent to "chaotic" states characterized by "strange attractors" in the modern theory of dynamical systems? What deeper insights can the theories of chaos bring to our dealing with turbulence in open flow systems and in particular to our engineering task of estimating the x-location of transition to turbulence? The 1988 Spring issue of a certain alumni magazine quoted an eager researcher at the university: "...we are now able to predict the point at which a laminar flow will start to become turbulent..." and "This applies to the turbulent flow encountered by any type of vehicle in any fluid". We note that the four-syndrome characterization of turbulence refers to localized regions of the shear layer and allows for turbulence to coexist in proximity with laminar flow as in both types of turbulent spots above. In the theory of dynamical systems the designation chaotic refers to the state of the whole system - the whole shear layer. Locating the x-onset "point" of turbulence in a vehicle boundary layer requires additional assumptions which should be rigorous. Swinney and Gollub (1986), who pioneered the experimental study of chaos in closed-flow systems, aware of such difficulties, state in a review article: "It is not yet clear whether the strange-attractor concept is useful for open systems..."

Before attempting to address the questions in the preceding paragraph, we need to clarify in Section 3 what is meant by convective, absolute and global instability in open-flow systems. A simple illustration of the concept of strange attractor and some philosophical implications of chaotic phenomena is found in the Appendix.

#### (2.6) $Re_{mint}$ , $Re_{cr}$ , $Re_{tr}$ , and bypass transition

Two more physical concepts which distinguish between intrinsically laminar flows and decaying turbulent flows are signaled in Fig.3. There is ample evidence, Morkovin (1984), that boundary layers below a Reynolds number,  $Re_{mint}$ , cannot sustain intrinsic self-energizing turbulent motions on the scale of the local shear layer thickness  $\delta(x)$ . In turbulent boundary layers, the unsteady energy dissipated near the wall is restored through intermittent "bursts" which produce negative Reynolds stresses  $-\rho \overline{u'v'}$  and recoup energy from the mean

flow. Two types of events associated with bursts, ejections and sweeps, are identified in Fig. 3. The ejections in particular have the character of local instability which evidently is absent below  $Re_{mint}$ .

Any locally forced turbulence, say by a spark or local separation, decays rapidly. Even when vigorous free-stream turbulence is convected toward the boundary layer as in Fig. 1a, the energizing "bursts" (with scales smaller than  $\delta$ ) are not excited. Rather, the boundary layer experiences some three-dimensional motions on scales larger than  $\delta$  and some mild increases in mean wall stress and heat transfer rates. However, the boundary layer remains intrinsically laminar. This randomly unsteady quality is conveyed by the term "buffeted laminar layer" in Figs. 1a and 3. For the given shear-layer geometry the earliest possible transition, important in design, occurs at  $Re_{mint}$ .

The observed minimum  $Re$  for self-sustained turbulence in four types of flows are compared to corresponding critical  $Re$  for first laminar amplification of infinitesimal disturbances in Fig. 4. In presence of moderate to small environmental disturbances of turbulence,  $Re_{tr}$  in boundary layers is generally observed downstream of  $Re_{cr}$ , at distances corresponding to inferred total amplifications of roughly 100 to 10,000 of the linearly most dangerous disturbance. The observed approximate coincidence of  $Re_{mint}$  and  $Re_{cr}$  of about 200 (based on momentum thickness  $\theta$ ) for the flat plate has remained unexplained for forty years. However, the expected sequence  $Re_{mint} < Re_{cr} < Re_{tr}$  is generally observed in boundary layers on bodies with finite thickness when disturbances are moderate.

Occasionally,  $Re_{tr}$  does not appear to be related to  $Re_{cr}$  and may even occur upstream of  $Re_{cr}$ . Obviously, such cases can play havoc with design, as it did in the humbling case of the heat-sink nose on the first reentry vehicles in 1956, Murphy and Rubesin (1966), Morkovin (1984). (This is called the blunt-body paradox in Fig. 15.) On blunt bodies at high speeds the transition path to turbulence bypasses to this day all known instability theories and documented mechanisms (although highly accelerated thin boundary layers are known to be very sensitive to surface roughness). We can expect large disturbances (local wall distortions, vigorous oncoming turbulence) to cause bypass

transition as outlined in Fig 11. However, the mildly disturbed "naturally occurring" bypass transitions  $Re_{mint} < Re_{tr} < Re_{cr}$ , in pipes and ducts in Fig.4 also remain unexplained. These flows are more subcritical to axisymmetric and two-dimensional disturbances than boundary layers (Section 2.3), but experiments point to three-dimensional disturbances and more subtle causation.

### (2.7) Relaminarization

The final important concept in the summary Fig.3 deals with relaminarization, which has been extensively documented and analysed by Narasimha and Sreenivasan (1979). One of the several relaminarization mechanisms they describe operates in highly accelerated turbulent boundary layers. The favorable pressure gradient increases dissipation near the wall and stabilizes the inner layer. The turbulence-re-energizing bursts diminish in frequency and stop altogether. A thin new laminar layer grows from the wall within the old boundary layer, which now decays and becomes wake-like. The outer-layer turbulence cannot stop instantaneously; it is merely "starved". In fact, the growing inner layer constitutes a laminar layer "buffeted" by the decaying turbulence of the outer layer. It remains so until it grows past its  $Re_{mint}$ , Sternberg (1954), or until the favorable pressure gradient is relaxed and bursts recommence. Again, the wall stress and the heat transfer rate in such relaminarized buffeted inner layers appear to be less than those expected in turbulent layers, justifying the term "locally relaminarized".

### 3. CONVECTIVE INSTABILITY AND STREAMWISE RESONANCE

#### (3.1) Local convective and absolute instability

The normal-mode responses to the specialized harmonic excitation of the linearized primary instability, Fig.2, were termed spatial or temporal. A more fundamental instability response of a shear layer is that to an impulsive forcing disturbance at  $t = 0$ , localized at the origin of the streamwise and spanwise coordinates. In terms of Dirac's impulse functions, response is desired to the forcing term  $\delta(t)\delta(x)\delta(z)$  on the right side of the otherwise homogeneous linearized stability equation. This search for a Green's function of the linearized system represents an idealization of the experiment of Gaster and Grant (1975). By repetitive excitation and judicious sampling these researchers measured the unsteady response of a Blasius boundary layer to short weak pressure puffs from a very small hole in a flat plate. At any time after the puff, the boundary layer was disturbed only over a small  $x$ - $z$  area which grew slowly in size as the disturbance field propagated downstream. In accordance with the filter-amplifier characteristics of the layer, the disturbance took the form of  $x$ - $z$  wave packets which grew at first nearly exponentially in amplitude within the disturbed, propagating "laminar spot". At later times nonlinearity and higher instabilities modify the nearly exponential linearized primary instability behavior. Such localized exponential growths within downstream propagating spots are defined as being convectively unstable.

Figure 5a, based on Huerre and Monkewitz (1985), and Huerre (1987) illustrates the linearized convective instability in one less dimension than the Gaster-Grant experiment. As in Fig.2 the response is exponential, but in both  $x$  and  $t$  simultaneously, yielding a growing wave packet within the propagation wedge shown in Fig.5a. Outside the wedge the factor  $\exp(\omega_i t)$  with  $\omega_i$  negative damps out the response. The wave packet transmits disturbance energy at the group velocity  $c_g = \partial\omega_r / \partial k_r$  which is associated with a ray  $x = c_g t$  within the wedge.

In some flows, illustrated in Fig 5b, the group velocity becomes zero and the disturbance energy remains centered on the point of impulse,  $x = 0$ . The disturbances then grow exponentially in place and disperse somewhat in  $x$  according to the normal-mode dispersion relation. Such linearized flows are called absolutely unstable. In open-flow systems, most of the mean vorticity of the shear layer continues to be convected downstream but the energy, associated with the vorticity disturbance field may be trapped, "working upon itself". We note paranthetically that this self-interactive character of the disturbance field is partially similar to the interactive conditions of Section A-4 for Couette and Bénard-Rayleigh flows, which ultimately lead to strange-attractor behavior. Those two flows are indeed absolutely unstable, but in addition they are closed with respect to the mean vorticity, an important feature when turbulence and phase jitter set in.

### (3.2) Linear resonance in $x$ , nonlinear effects and pressure feedback

The spot-like character of the impulse response requires both the circular frequency  $\omega$  and the wave number  $k$  (often denoted by  $\alpha$ ) to be complex in the spatio - temporal factor  $\expi(kx - \omega t)$  in Fig. 5. A functional relation  $\omega(k)$  (the dispersive relation in terms of the flow parameters) is imposed by linearized equations for the disturbance in the given flow. The absolute instability condition  $\partial\omega/\partial k = 0$  of zero group velocity generally corresponds to a double root for the eigenvalues of  $\omega$ . Two disturbance vorticity waves propagate then at the same speed  $\omega_r/k_r$  and potentially could "resonate". Koch (1985) postulated that vanishing of the  $\omega$  derivative in the wake of a bluff body indeed corresponds to a resonance leading to the extra strength and regularity of the observed Karman-Benard vortex street. The resonant-like nonlinear regularity of the Karman-Bénard street is now believed to be associated with global instability of the flow, Monkewitz (1988), for which the initial absolute instability is only a necessary but not a sufficient condition, see Section 3.4.

The important definitions of convective and absolute instabilities are strictly valid only for small-disturbance linearized flows which

are independent of  $x$ . The extra qualifying adjective "local" for these instabilities underscores the suppression of the  $x$  dependence of the layer in the analysis, which then permits separation of variables and reduces the problem to the search for eigenvalues in  $y$ . Wakes of bluff bodies and jets with variable density (the other open-flow shear layer with absolute instability, Monkewitz and Sohn, 1986) unfortunately exhibit rather strong  $x$ -dependence and depart significantly from infinite parallel layers. Furthermore, the suspected resonance involve wave interaction in  $x$  with some unspecified reflection at the body and possibly elsewhere.

In the bluff-body cases, the local instability criterion disregards completely the strong destabilizing adverse pressure gradient near the base which is suspected to contribute significantly to the magnitude of the pressure fluctuations. It is known that the common dominant low-frequency pressure disturbances in wind tunnels stem from irregular separation in diffusors with adverse pressure gradients. Instantaneous separation lines often tend to be nonuniform spanwise due to presence of  $\omega_x$  at moderate Reynolds numbers. However, resonances in  $x$  in shear flows tend to straighten out separation lines and lead to still larger fluctuations. There is nonlinear hydroacoustic feedback to upstream regions which reinforces or modifies any interactions (and feedback tuning) between vorticity waves.

In other words, the shear layer we observe may differ substantially from the hypothetical ones in which infinitesimal disturbances presumably initiated the resonant processes. For instance, at  $Re_D \sim 120$  the streamwise velocity fluctuation  $u'$  in a cylinder wake exhibits the nonlinear level of  $0.02U_\infty$  right at the separation of the shear layer from the body, Nishioka and Sato (1978, Fig. 5). The pressure fluctuations seeded by the vigorous nonlinear vortex formations (see equations in Fig. 7) actually reach upstream of the cylinder and precondition the boundary layer on the cylinder upstream of the oscillating separation point. This exceeds any upstream effects which a vorticity wave interaction-resonance could have caused at the initial linearized level and is therefore unquestionably hydroacoustic in character. The same Nishioka-Sato figure documents that this case of local absolute instability (characterized by the purely temporal



initial instability in Fig. 5b) evolves into a global instability in the form of a rapid purely spatial  $u'$  amplification in  $x$  for  $x/D$  up to approximately 2.5 and a slow decay thereafter. The maximum fluctuation  $u'$  (in excess of  $0.3U_\infty$ ) is located just downstream of the closure of the mean-wake recirculation pocket. This provides support for at least a contributory role of vorticity feedback in the final state of cylinder-wake resonance at low Reynolds numbers.

The resonant bluff wake has an additional property, useful in diagnostics. It is robust with respect environmental disturbances. In other words, the nonlinear feedback system filters out external perturbations to the point that the Re-dependent frequency of the vortex street has been used successfully for velocity measurements at low speeds where Pitot tubes are inaccurate, Roshko (1955). The resonant near wake at low Re seems to have just two effective degrees of freedom and behaves like a second-order Van der Pol oscillator with a robust limit cycle described in Section A-2 and Fig A-1a,b.

### (3.3) Noise response of convectively unstable layers

Figure 6 summarizes the progression of idealizations leading to a model of nonlinear global instability, presumably mimicking the resonance of the cylinder near wake. First, for the linearized convectively unstable shear layer - present in the majority of open flows - the local parallel approximation exacts no significant penalties. Second-order nonparallel theories (when carried out correctly) provide relatively small correctons for  $Re_{cr}$  and amplification rates. The convective character of the instability remains unchanged.

Thus by definition of convective instability each successive disturbance "received by the layer from upstream" generates its own laminar spot which propagates downstream as it grows exponentially. In wind tunnel environments with continuous randomly modulated disturbances laminar spots tend to superpose while maintaining some random phase and amplitude nonhomogeneity in  $x$  and  $z$ . Sampled at any frequency within the amplified spectrum, the response resembles that of an averaged quasi-two-dimensionally spatially growing unstable wave;

see lower half of Fig.13. As these disturbances approach nonlinear levels, the amplified, noise-sustained structures (in the language of Deissler and Kaneko, Section A-4) are ready for secondary and higher instabilities, fed in part by the amplitude inhomogeneities in  $x$  and  $z$ .

The convectively unstable shear layers lack any robustness with respect to environmental disturbances - on the contrary they are driven by them, probably even quite some distance into the fully turbulent region. The randomness and nonhomogeneity of the response is reflected in an extended region  $\Delta Re_{tr}$  within which the local onset of turbulence may take place. This is illustrated in the lower half of Fig. 13, where  $Re_{tr-beg}$  refers to the upstream position of the onset and  $Re_{tr-end}$  to the location past which all activity near the wall is burst-like, Section 2.6. Measured ratios  $\Delta Re_{tr}$  to mean  $Re_{tr}$  in wind tunnels are often on the order of 0.4, but tend to be smaller in adverse pressure gradients.

The vision of transition prediction by the researcher quoted in Section 2.5 is thus strongly contraindicated for convectively unstable boundary layers "on any vehicle".

#### (3.4) Absolute versus global instability

Local absolute instability rests on the character of the eigenvalue problem in  $y$ . The occurrence of zero group velocity in the  $x$ -dependent shear layer signals merely the possibility of a resonance in  $x$ . The visual evidence of Thorpe (1971, Figs, 1, 5 and 7) for the anti-symmetric mixing layer demonstrates a lack of robustness in his absolutely unstable flow. Unquestionably there is no resonance. The layer responds irregularly to the initial nonhomogeneities, which are amplified into "noise-sustained" saturated structures, and proceed to irregular pairing and sporadic onset of turbulence. It would almost seem that the very lack of  $x$ -dependence in the mean mixing layer (in contrast to that of the bluff near wake) removed "the opportunity" for resonance, such as partial or full reflections of the vorticity waves.

The situation seems to have been clarified on a partial differential equation model (the Ginzburg-Landau equation in  $x$  and  $t$ ,

with a convective term  $U\partial A/\partial x$ , a cubic nonlinearity and one coefficient slowly varying in  $x$ ) by Chomaz, Huerre, and Redekopp (1988). The linearized equation admits an undamped eigenfunction in  $x$  - a robust global instability - only when the  $x$ -extent of the equivalent local absolute instability reaches a finite critical size. Numerical solutions of the full nonlinear equation for impulsive white-noise conditions exhibited the successive behavior for the stable, convectively unstable, absolutely unstable, and globally unstable regimes as the parameter of the system was varied.

Monkewitz (1988) in his study of local viscous linearized stability of a family of wake profiles associated the onset of the three unstable stages with  $Re_D$  of approximately 5, 25, and 47, respectively. He took the empirical result for the spontaneous onset of the oscillations at  $Re_D \sim 47$  as the criterion for the onset of global instability, a criterion not obtainable in parallel approximations. The common absence of oscillations in the convective regime  $5 < Re_D < 25$  is ascribed to the absence of environmental disturbances in the narrow excited range of frequencies. Taneda's 1963 visualizations of wakes downstream of slightly vibrating cylinders supports this interpretation; see discussion of Fig. 5 in Morkovin (1964).

Judging by Fig. 16 of Nishioka and Sato (1974) for the recirculating wake, Monkewitz local conditions for absolute instability at  $Re_D \sim 25$  correspond to the closure of the steady recirculation pocket at  $x \sim 1.7D$ . Just below the spontaneous street onset at  $Re_D$  of 47 the pocket extends to  $x \sim 3.1D$  and presumably provides the increased critical range needed for the resonance in  $x$ . Just as in the model of Chomaz et al (1988) in this regime of absolute instability there is little qualitative distinction of behavior from that in the convective instability regime: external forcing is required for the instability to appear and grow. For instance minute cross-flow oscillations of the cylinder engender an initially linearizable exponential amplification in  $x$  for  $Re_D$  of 30 and 40, as documented in  $x$  in Figs. 6 and 7 of Nishioka and Sato (1978).

Altogether, the picture now appears rather consistent despite the ambiguities, outlined in Section 3.2, associated with the definition of

local infinitesimal instability, the usage of mean profiles in highly disturbed flows and the role of the nonlinear hydroacoustic feedback. Particularly convincing were papers which studied the time evolution of the global instability after it was suddenly "switched on" and which verified that the whole field grew temporally with the single factor  $\exp(\omega_{i0} t)$  in the linear regime, as one would expect from Fig.5b. Experimental analytical verification came from Sreenivasan, Strykowski and Olinger 1987 and Provensal, Mathis, and Boyer (1987), while a numerical study for a thick flat plate with a square base was described by Hannemann and Oertel (1987), based on Hannemann's dissertation.

The numerical experiments permit detail examination of some of the aforementioned ambiguities. In accordance with the scenario of Chomaz et al (1988), Hannemann (1988, Fig. 42) finds the flow damped at  $Re_D = 80$ , where the range of local absolute instability extends from the base to  $x = 2.3D$ , a range evidently insufficient to build up an amplifying eigenfunction in  $x$ . For  $Re_D = 200$ , the disturbances in a quasistationary symmetric Navier-Stokes field grow everywhere by a factor of  $10^5$  in accordance with the linearized factor  $\exp \omega_{i0} t$  while the free stream covers a distance of about  $240D$ . The subsequent nonlinear evolution, starting at  $u' = 0.007 \cdot U_\infty$  is marked by (1) gradual shortening of the mean recirculation pocket by eddy entrainment (Fig. 20), (2) change in mean velocity profiles, (3) a 10% increase in the Strouhal frequency (Fig. 21), (4) evidence of hydroacoustic feedback to the boundary layer upstream of the base, (Fig.28), and (5)  $\exp(2\omega_{i0} t)$  growth of a varicose instability component of twice the frequency of the initially pure sinuous instability and movement of the unsteady vorticity maxima off the center line, (Figs. 24 and 19).

### (3.5) Convective-hydroacoustic global instability; numerical simulations

In closing this section, we should note that a whole class of global instabilities of free shear layers is sustained by hydroacoustic feedback when they impinge on a solid boundary; see bottom of Fig.6 and the overview by Rockwell and Naudascher (1979). When unsteady vorticity of a convectively unstable free shear layer impinges on a wedge, it generates pressure feedback to the point of separation of the

layer. Receptivity to unsteady pressures gradients at separation being very high, Morkovin and Paranjape (1971), significant unsteady vorticity is generated at the origin of the layer. This newly-born unsteady vorticity is amplified by the unstable shear layer and convected toward the wedge, thus completing the resonance loop. A singing teakettle commonly reminds us shrilly that such loops can build up substantial energy levels. There is resonance and at least one undamped eigenvalue in  $x$ ; there is robustness with respect disturbances (except for conditions of competition between two neighboring eigenvalues).

The nonlinear generation of unsteady pressure is absent when Hannemann's global bluff-wake instability commences. But his Figure 28 indicates that the upstream effects of the pressure grow with nonlinearity and that they probably contribute to vorticity control at the very origin of the wake in the later stages of the global instability at low Reynolds numbers discussed here. At high  $Re$  values the threshold for pressure feedback maybe very low.

It is worth noting that the upstream traveling vorticity or pressure wave can be decaying in the negative  $x$  direction and yet sustain the global resonance. In the hydroacoustic case the pressure fluctuations decay in all directions from their origin, the exact manner depending on the geometry and the ratio of the total propagation distance to pressure wavelength (near-field versus far-field behavior). However, high receptivity followed immediately by large amplification in the layer and rather efficient conversion into pressure fluctuations at impingement, Rockwell (1983), provide sufficient regeneration and phase coherence to maintain the loop against more incoherent disturbances. We note that in the near-wake and variable-density-jet cases, the nature and dynamics of the resonant vorticity waves have not yet been identified theoretically or experimentally. The dominance of the spatial development, evident in the saturated state of the instability (Hannemann, 1988, Fig. 28; Nishioka and Sato, 1978, Figs. 4 and 5, Unal and Rockwell, 1988a, Fig. 5) suggests that any upstream traveling vorticity mode may be dwarfed in the interactions and may possibly be decaying towards the separation point.

Paradoxically, accuracy of numerical experiments with streamwise amplification of free shear layers is endangered by inadvertent pressure feedback from the unavoidable conditions at the outflow boundary, OB. Ideally, differential relations could be imposed at OB by dropping the "viscous" highest order derivatives from Navier-Stokes equations. This would make OB transparent to oncoming vortical structures except for a thin unsteady viscous "shock-boundary adjustment layer" just upstream of OB. (This BC scheme has convergence and expense problems). Otherwise, constraints imposed at OB convert the convected dynamic field more or less efficiently to pressure fluctuations as in the case of impinging shear layers. Pressure feedback to the receptive separation region of the layer and subsequent amplification-convection provide an additional disturbance loop imposed upon the "natural" dynamics of the layer under scrutiny. From the computed results alone, it is difficult if not impossible to judge how serious the likely modifications of the dynamics may be - changes in phase, amplitude, frequency, wavelength, onset of higher instabilities, etc.

Simpler differential conditions at OB with some promise are

$$\left\{ \frac{\partial}{\partial t} + U(y) \cdot \frac{\partial}{\partial x} \right\} \underline{V} = 0 \quad \text{or} \quad \left\{ \frac{\partial}{\partial t} + U_c \cdot \frac{\partial}{\partial x} \right\} \underline{V} = 0$$

where  $U_c$  is a convection velocity of large eddies near OB and  $\underline{V}$  the velocity vector. They correspond to Taylor's hypothesis in hot-wire anemometry and presumably decrease conversion of the energetic eddies into pressure fluctuations. The condition  $\partial^2 u / \partial x^2 = 0$  used by Hannemann is adequate for low-amplitude vorticity waves in attached boundary layers with low receptivity, but its applicability to free shear layers with separation should be rigorously investigated. A similar problem, though probably less serious arises at the inflow boundary, IB. The practice of prescribing specified  $y, t$  or  $y, z, t$  velocity variations on IB may simulate tolerably the vorticity or pressure waves which penetrate the field of computations from upstream. However, since these prescribed values do not allow for any modifications by pressure fields spreading from within the computing domain or from OB, the condition automatically imposes a complicated velocity mode at IB, tantamount to special spurious reflections.

#### 4. NATURE AND ROLE OF RECEPTIVITY

##### (4.1) Receptivity-conditioned weak global instability in mixing layers

In Section 3.5, we saw how a convectively unstable free shear layer can be converted into a globally unstable system by inserting into it a solid object which generates unsteady pressure feedback to the separation region. In its initial laminar segment many a mixing layer has the character of a weak global unstable system without intervention of an intruding body: the vigorous vortex pairing driving its secondary instability replaces the impingement region as the pressure source. Figure 7 summarizes the many coupled processes involved in the complicated two-frequency feedback loop as documented by investigators at the Illinois Institute of Technology: Drubka (1982), Shakib (1984), Corke (1987), Corke, Shakib and Nagib (1988).

The observation that downstream large-scale vortex structures in a mixing layer, even turbulent ones, may modulate the primary instability near the lip came from Dimotakis and Brown (1976). Laufer and Monkewitz (1980) focused on the feedback due to pairing, but the complex coupling loop in Fig 7 was deciphered at IIT. The reader is referred to Ho and Huerre (1984) for a rewarding description of the rich variety of other stability-related phenomena in initially laminar mixing layers. The IIT evidence consists of simultaneous measurements of unsteady pressure on the vertical flange above D in Fig 7, velocity fluctuations sensed by a hot-wire movable along and across the layer and of various combinations of processing of both signals. Although we shall outline the developments in terms of single-wire data in the inset on the right of Fig 7, the chicken-egg reconstruction of the system rested ultimately on two-point correlation, coherence and bicoherence functions of pressure and velocity.

At the start of the layer in a sound-insulated low-disturbance facility the  $(u')^2$  velocity spectra are broad-band, almost without peaks, indicating absence of spurious acoustic or vibrational disturbances and the weakness of the feedback. The rise of the first

two feedback-initiated frequency peaks is sketched in the inset of Fig 7. Both the logarithmic slopes agree well with the linearized spatial amplification rates computed by Monkewitz and Huerre (1981) for the primary instability. The puzzling fact that the strongly amplified fundamental of frequency  $f$  is generally 15-25% slower than the theoretically strongest amplified frequency  $f_m$  was first mentioned to the author by A.K.M.F. Hussain ten years ago. Also initially surprising was the fact that its subharmonic at  $f/2$  started at a level about an order of magnitude higher, see D in inset. The probable answer appears to be first that the nonlinear interaction of the combinations may extract energy more efficiently from the mean flow than the  $f_m, f_m/2$  combination. Secondly the relatively high initial  $f/2$  level stems from the fact that vortex pairing is vigorous and generates higher pressure fluctuations than the more gradual vortex roll-up of the primary instability. The proximity of the latter to the lip is compensated for, since the pressure decay from a pairing multipole scales with wave length and therefore lower frequencies reach farther. The low Mach number equation for generation of the feedback pressure is shown at the top of Fig 7. The conversion into vorticity fluctuation is proportional to the spatial gradient of the pressure around the lip, not the pressure level, Morkovin and Paranjape (1971). Sharpness of the corner causes a large local increase in  $\partial p/\partial s$ , thereby enhancing receptivity at separation.

Up to the position  $A^*$ ,  $f$  and  $f/2$  develop independently, propagating at different speeds close to those of linear theory. At  $A^*$  a nonlinear threshold is reached where the subharmonic locks onto the speed of  $f$  and can thereby extract energy through the fundamental. This corresponds to the onset of the secondary parametric instability of Section 2.3: the subharmonic grows now exponentially at the linearized rate associated with the new base flow of rolled up vortices A and B of the fundamental. The subharmonic saturates at C, roughly at the position where the two strained vortices pass each other in  $x$  and manifest largest gradients  $\partial u_i/\partial x_j$  before viscous vorticity diffusion



cuts them down. (The products of the gradients in the source for the pressure fluctuations are summed on  $i$  and  $j$ .)

This double-frequency, globally unstable system was called weak because the fluctuation level at separation remains low, roughly hundred times smaller than that at the Nishioka-Sato separation on the cylinder, at  $Re \sim 120$ , described in Section 3.2. Edge-tone systems also pump themselves up to higher energy levels since dipole impingement sources are more efficient than the quadrupole sources in the pairing process of Fig 7. The strength of this compound mixing-layer oscillator is clearly limited by the saturation levels it can sustain. It can be disorganized by environmental disturbances and by artificial pressure fluctuations once these exceed sufficiently the initial levels of the fundamental and its subharmonic at D.

#### (4.2) Noise amplification in mixing layers

The coexistence of independent linear development of  $f$  and  $f/2$  in the range  $DA^*$  illustrates the important fact that the mixing layer can amplify simultaneously (albeit at different rates) frequencies from zero to about  $U/2\delta$  if imprinted at D. Only when the most prominent oscillation reaches sufficient nonlinear levels it may strengthen (or inhibit) other frequencies, such as the subharmonic at  $A^*$ . This is effected through higher-order instabilities, often of parametric nature when frequency ratios are rational numbers, see Section 2.4. Further details on the richness of such forced nonlinear behavior in mixing layers are found in Ho and Huerre (1984).

Two consequences follow. First, low-frequency vorticity waves often permeate the shear layer, imprinted upon it at the origin by stream turbulence, irregular pressure fields, and feedback from large-scale downstream turbulent structures, Dimotakis and Brown (1976). At low amplitudes, their structure is little modified by the smaller-scale secondary instabilities, which they "modulate". After the layer thickens enough for them to acquire higher amplification rates they suddenly become active in a higher-order instability of their own. Sutton et al (1981) demonstrated the effect by vibrating

the separation point; the behavior persisted into the turbulent regime! It seems that a mixing layer, in contrast to the boundary layer, almost never forgets its long-wavelength vorticity structure.

The second consequence is that extrinsic noise in a mixing layer will generate amplified, mildly filtered, noisy structures in accordance with the Ginsburg-Landau model of Deissler and Kaneko (1987). Thus, because its global instability is weak and limited to a short initial stretch, a mixing layer behaves quintessentially as a convectively unstable system, even when turbulent; see also Fiedler et al (1985). If a strange attractor existed for this x-dependent layer, its intrinsic irregularity would be contaminated by the extrinsic stochastic noise amplified by the layer.

#### (4.3) Illustration of unsteady forcing of boundary layers

In Section 2 we discussed unstable vorticity restructuring, assuming that vorticity nonhomogeneities were already internalized in the shear layer. In Section 4.1 and Fig 7 we described the manner in which an unsteady pressure gradient is converted into an unsteady internal vorticity wave at the origin of a mixing layer. This is a case of a strong very localized receptivity, proportional to  $\partial p/\partial s$  around the lip, with coefficients depending on the exact geometry and the forcing Strouhal number,  $f\delta/U$ . Next we examine a layer without any separation or twodimensional leading edge.

Figure 8, courtesy of Kegelman (1982 thesis at Un. of Notre Dame), displays visual evidence of the excitation of TS (Tollmien-Schlichting-Schubauer), the viscosity-tuned waves on an ogive-cylinder model (see inset) by sound from a loudspeaker upstream of an open-throat wind tunnel at levels of 105-115dB. The smoke from an upstream source impinged symmetrically on the sharp nose and made the forced unstable waves visible some distance past the shoulder. Diagnostics with a hot-wire anemometer showed that the self-excited wave-pattern response to the forcing sound field began building up from the oscillatory Stokes layer just upstream of the ogive-cylinder junction, where no

imprint on the smoke is yet visible. The range of excitation frequencies from 551 to 785 is impressive for an attached boundary layer. The spanwise inhomogeneous break up, featuring  $\Lambda$  vortex formations are now identified as H and occasional K secondary instabilities, Herbert (1988), as described in Section 2.3.

Figure 8 demonstrates beyond doubt that harmonic forcing by unsteady irrotational fields generates early unsteady rotational waves in convectively unstable shear layers. Clearly, transition to turbulence cannot be predicted without the knowledge of the forcing field (frequency, amplitude, orientation), the dominant receptivity mechanism, and the threedimensional inhomogeneities of vorticity internalized in the boundary layer from other environmental disturbances. Even though the Reynolds number is the same in Fig 8, the turbulent boundary-layer structures over the body appear to be governed by the above factors. Any more universal asymptotic features, if they could develop, evidently would require longer evolution.

Of the three factors limiting the predictability of transition to turbulence, the receptivity mechanisms to harmonic pressure forcing such as that in Fig 8 have recently undergone considerable clarification. They will be discussed in conjunction with Fig 11 in Section 4.6.

#### (4.4) On forcing of shear layers by quasisteady fields: Goertler instability

Forcing by steady  $\omega_x$  vorticity fields and surface roughness has been largely ignored in the literature. And yet it is the primary source of the threedimensionality in secondary instabilities. Composite Figure 9, based on wind-tunnel experiments of V. Kottke (1986), illustrates the forcing of steady-in-the-mean Goertler vortices in a concave boundary layer (right side of Fig 2) by a primarily unsteady vorticity generator, namely the grid with mesh M and rods of diameter d in upper Fig 9. Kottke (1980) and colleagues, e.g. Kottke

and Schmidt (1985) developed a chemical method for flow visualization in a wind tunnel and simultaneous photometric determination of local mass transfer rates. Grids and honeycombs bring forth complex threedimensional, multiply unstable and x-decaying wakes, Loehrke and Nagib (1972), (1976), which have been used for both generation as well as decay management of freestream turbulence. The curvature of Kottke's plate is relatively large so that in the parameter range of Fig 9 its boundary layer remains a buffeted laminar one, Section 2.6. However, the boundary layer is susceptible to centrifugal instability and responds to the mean-flow nonuniformities, which are invariably present (though seldom mentioned or documented) in flows with higher turbulence.

The second row of Fig 9 demonstrates how the streamwise vortices form readily when the grid distance  $x_g$  from the plate leading edge is small. As  $x_g$  increases the mean streamwise vorticity  $\omega_x$  entering the concave boundary layer (or induced within it) subsides and so does the strength of the Goertler vortex response. In the third row of Fig 9, the grid distance is held fixed, but the mesh  $M$  is varied, eliciting a wave number response in limited qualitative agreement with "parallel" linear theory for  $M \gg 7$ . The quantitative inference on the right of Fig 9 of the local and (spanwise) mean mass transfer coefficients  $\beta$  and  $\bar{\beta}_z$  in m/h supplement the visual information.

Clearly, the forcing by mean "environmental"  $\omega_x$  distributions feeds the development of the centrifugal instability and predictions without better knowledge of the oncoming disturbances and the associated receptivity paths will prove fictional and wishful. For this flow, the critique of the formulation of the linear instability theory itself by Hall (1982), (1983) compounds the predictive difficulties. Fortunately, recent and ongoing judicial application of the numerical marching technique of Hall by Kalburgi, Mangalam and Dagenhart (1988) and others restores considerable engineering utility to the results of the linear theory of Floryan and Saric (1984).

Amplitude resolution of measuring techniques for steady  $\omega_x$  fields

is orders of magnitude inferior to measurements in unsteady fields which are aided by the electronic amplification. Thus the comparison between linear theory and experimental results (many detected only at the nonlinear level) has always remained ambiguous. The net evidence points to strong imprinting by the particular  $\omega_x$  distribution in each facility. In other words, the system is not robust with respect to disturbances, despite Huerre's 1987 conjecture that the system is absolutely unstable.

In the experiments of Kottke in Fig 9, only the effects of the primary instability are evident. Secondary unsteady instabilities, symmetric, sinuous and others have been studied experimentally only recently, and are burdened by the uncontrolled nonuniformities of the saturated primary field. For some results and guide to earlier literature see Swearingen and Blackwelder (1987).

Figure 10, middle, singles out two often neglected sources of quasisteady forcing of boundary layers: nonuniformities in leading edges (especially at supersonic speeds) and surface protuberances or dimples. Obviously the resulting local pressure gradients cause local cross-flows and  $\omega_x$ . At the author's suggestion Wilkinson placed a small intentional roughness element on the surface of a rotating disk and demonstrated in great detail that the well-known growing spiral vortices were driven by it, Wilkinson and Malik (1985). This forcing experiment carries special significance because Mack (1984) was able to reproduce to a remarkable degree the wave patterns and growth on the basis of linear theory, thus verifying this path of receptivity.

Quasisteady forcing of instabilities is equally important in free shear layers: any  $\omega_x$  disturbance entering the layer at the separation line where it is born governs subsequent evolution of its threedimensionality. Recent evocative visualization and discussion of the effects can be found in Lasheras and Choi (1988).

(4.5) Environmental forcing in open-flow systems

Most open-flow systems of technological interest are convectively unstable, Section 3 and Fig 6. Therefore small environmental disturbances do energize and amplify the numerous competing intrinsic unstable modes in all primary and higher-order instabilities leading to turbulence. These external disturbances can be classified, Fig 10, as: (A) irrotational unsteady pressure fields (sound, including near-field of pseudosound) which travel across streamlines, (B) threedimensional vorticity fields (usually decaying remnants of turbulence from upstream shear layers), convected with the mean motion of the fluid, while nonlinearly diffusing; (C) unsteady threedimensional entropy-temperature-density (ETD) spottiness of Kovaszny (1953) also convected "parabolically" from upstream mixing of shear layers of unequal temperatures; (D) steady-in-the-mean streamwise vorticity  $\omega_x$  and ETD patterns, (present in all ground facilities but undetectable directly because of the exceedingly poor resolution of  $\omega_x$  detectors; these fields force cross-flow instability and Goertler instability responses; (E) particulates and aerosols (including dust) in the fluid which individually and collectively cause flow nonhomogeneities along their nonequilibrated paths through the shear layer, e.g. Lauchle and Gurney (1984). In addition, (F) vibrational motions of any walls in the system and (G) nonhomogeneous or unsteady heating of such walls often provide significant seeding of instability modes (which may explain some anomalies in past observations).

Because they are generally small, the disturbances are very hard to identify. Even with two independent instruments, the distinct irrotational velocity (pressure) fields and the rotational (laminar or turbulent) velocity fields have never been adequately resolved in any facility. The best calibrations of wind tunnels, such as that of Winter and Maskell (1980) leave hosts of unanswered questions as to the actual forcing fields. For practical purposes we don't know and are unlikely to know the input freestream disturbances into our unstable shear layers. In fact, they are not fixed and change during any test and from test to test. Philosophically, this reality must be

accommodated in any rational "prediction scheme" - perhaps by plausible bracketing estimates.

The freestream fields, however, undergo straining and distortions by any solid boundaries, Fig 1, Receptivity paths are to be sought with respect to the strained fields, which often are more effective. In fact, it is the straining of the sound field in Fig 8, which enables the seeding of TS waves despite the disparity in wavelengths between the sound and vorticity waves of the same frequency. The straining provides new characteristic lengths commensurate with the TS wavelengths. Much remains to be done in the matter of straining of vorticity and sound fields as related to receptivity paths. At supersonic and hypersonic speeds the interaction of these fields with body shock waves creates additional unsolved problems.

Various other issues and problems are listed in Fig 10; they are essentially selfexplanatory. The overall perspective provided by Fig 10 is sobering with respect to predictability of turbulent onset in open-flow systems. One implication points to the futility of judging the environmental disturbances by the single parameter  $u'/U_\infty$  at a fixed point, which is incorrectly identified as turbulence level. General correlations of transition based on this number have the scientific validity of schemes for choosing lottery numbers. When  $u'/U_\infty$  exceeds 0.5% or so, prospects of establishing reliable trends with various parameters are slim. Levels below 0.1% (including low-frequency contributions) are considered necessary for serious research on transition. In contrast experiments on controlled primary instabilities are considerably less sensitive to external disturbances.

#### (4.6) Receptivities to unsteady pressure fields

The conversion of environmental unsteady pressure fields into unstable vorticity waves, such as displayed in Fig 8, has been subject to numerous experiments, with rather contradictory conclusions. The more significant experiments were summarized and critically reviewed in

Sections 1 and 5 of Nishioka and Morkovin (1986). The same paper describes the results of a more controlled experiment on acoustic irradiation of a Blasius boundary layer at unstable, neutral, and stable TS frequencies. As noted in the preceding section, the mismatch between the TS and acoustic wavelengths (or equivalently between the TS and sound propagation speeds) tends to make this receptivity rather poor.

Receptivity improves as additional effective characteristic lengths are introduced into the combined system of the forcing, diffracted acoustic field and the boundary layer. An infinite Poiseuille-duct flow has zero linear receptivity to a uniform harmonic pressure gradient in the duct. Both flow solutions, being uniform in  $x$ , simply superpose without interaction. Variations of the amplitude of the unsteady pressure gradient with  $x$ , as in Fig 8, and variation of the boundary layer thickness with  $x$  provide two specific receptivity paths; see Nishioka and Morkovin, Sections 2 for the physics of the interaction and Section 5 for other receptivity paths. Because of the lack of controlled experiments, the question of which paths are most efficient for a given geometry remains open.

Depending on geometry the seeding of TS waves may take place over a short segment of the boundary layer, shorter than one TS wavelength. Such localized receptivity paths lend themselves to efficient analysis based on the triple-deck approach; see review by Goldstein (1986). On the other hand, extended distributed contributions to the TS vorticity strength do occur frequently over bodies with continuous curvature. The analysis is then complicated by positive and negative phase interference effects.

The left side of Fig 11 outlines the formal solution for the forcing, i.e. for the nonhomogeneous differential equations system. In principle, it depends on the completeness of the eigenfunctions for the system, such as proved for the Orr-Sommerfeld equation by Salwen and Grosch (1981). It was carried out explicitly by Bechert (1988) for the simpler inviscid case of a vortex sheet downstream of a semi-infinite plate and buttressed by the low-frequency experiments of Bechert and



Stahl (1988).

The familiar resonant vibrations of a wine glass in response to the excitation of a singer's voice will illustrate both the similarities and differences with the forcing behavior in an unstable boundary layer. The forcing fields evoke particular solutions of the nonhomogeneous linear differential equations governing the forced system. To these we can add any number of solutions of the homogeneous unforced system with arbitrary coefficients, the normal modes or eigensolutions. The requirement that the superposed particular and normal-mode solutions satisfy the complete boundary conditions over the boundaries of the wine-glass or the shear layer generally fixes the coefficients of the eigensolution spectra and thus selects quantitatively the response to the excitation.

In the case of the wine glass the vibrational eigensolutions are all frictionally damped and the response consists primarily of the particular solution; it is essentially proportional to the sustained amplitude of the singer's tone. Once the tone ceases, the response rapidly decays. In the rare cases when the resonant response amplitude exceeds a nonlinear threshold, the properties of the physical system are no longer governed by the idealized linear differential equations and the glass breaks.

The corresponding Nishioka-Morkovin experiments with a very weak sound source in proximity of a Blasius boundary layer demonstrated that when the TS waves at the exciting frequency were damped according to the linear Orr-Sommerfeld equations, a behavior ensued, similar to that of the wine glass. At each  $x, z$ , the response consisted of a finite-wavelength oscillatory viscous Stokes field in  $y$ , (the particular solution) plus small contributions from the damped eigensolutions. However, when the forcing frequency was in the spectral domain of amplified normal modes, the cumulative response grew in  $x$  very much faster (!) than allowed by the theoretical amplification

rate  $\alpha_i$  of the unforced normal modes. Once locally excited, these TS waves propagate downstream and continue to grow even if the periodic excitation ceases - in sharp contrast to the case of the wine glass. This is of course the behavior expected in a convectively unstable layer, inferable from Fig 5. As in the case of excitation by a vibrating ribbon, the propagation field becomes that of the amplified homogeneous normal mode. The key difference is that its amplitude is not arbitrary (as in linear stability theory) but set linearly by the amplitude and geometry of the forcing sound field, i.e. by the net receptivity for the configuration.

When the unsteady pressure field is not periodic, the linear mathematics becomes more involved, but the some principles govern the seeding of the amplified disturbances which are convected downstream within an unsteady laminar "spot". Kendall (1987) induced a traveling pressure wave as a cylinder approached and receded from a flat-plate boundary layer. The resulting complex amplifying pattern was documented through simultaneous measurements with multiple pressure sensors at the wall and hot-wire anemometry in the layer. The findings are consistent with the concepts described in this section.

#### (4.7) Unknown receptivity paths

When the external disturbances are large, additional nonlinear receptivity paths appear. They remain uncharted except for a few cases of high-level sound excitation, Ginevskii et al (1978). The bypass roads to turbulence, discussed in Section 2.6, by definition fall in the category of unknown receptivities. The right side of Fig 11, lists the more important cases and conjectures that local and/or transient inflectional shear-layer profiles may be responsible for the rapidity of the turbulence onset. Gill (1965) calculated that such an effect could be responsible for the transition in the linearly stable plane Couette flows and pipe flows.

However, unknown linear receptivity paths provide the conceptually more important challenges. Although Fig 9 demonstrated forcing of

Goertler instability by quasisteady  $\omega_x$  distributions, the corresponding linear receptivity mechanisms remain unknown. Similarly the forcing paths of the steady cross-flow instability as well as of the threedimensional traveling waves in threedimensional boundary layers have not been discussed in the literature.

Perhaps the most vexing and technologically important is the puzzle of receptivity to low freestream turbulence. Both experimentally and theoretically this is the most difficult linear receptivity problem. As noted on the left of Fig 11, any analysis performed using averaged quantities would solve the wrong problem. Almost of necessity, experimenters must use space-time correlations and coherences between multiple sensors. The difficulties far exceed those of known traveling wave fields of Kendall (1987) at the end of Section 4.6.

Hot-wire evidence: Bennett (1953), Arnal and Juillen (1978), Klebanoff (unpublished, 1964) and intriguing visualization in adverse pressure gradients by Gates (1980) imply that the receptivity path for low-intensity turbulence includes TS wave-packet formations, as the convective nature of the instability would suggest. Kendall's more controlled experiments (1984, 1985) with more extensive up-to-date instrumentation do indeed disclose energy in the TS bands (with decreasing frequency of the broadband peaks as the layer grows in  $x$ ). However, serious questions remain whether this path represents a weak ineffective sideshow while some threedimensional instability governs the dominant road to turbulence.

For further discussion of two possible ways of internalization of the external vorticity disturbances see p. 256 of Nishioka and Morkovin (1986) based on the implications of the cited research of Arnal-Juillen, Klebanoff, and Kendall. It is quite possible that the receptivity paths may depend on the specifics of the oncoming low-intensity, decaying turbulent wave packets in any given realization and on the straining fields associated with the flow facility and the front of the body including those at sharp leading edges.

Finally, a curious hybrid case is noted at the bottom of Fig 11. Unexpectedly, moderate distributed roughness which might disorganize TS waves, accelerated (!) the TS wave formation and secondary instabilities, Corke, Bar-Sever and Morkovin (1986). These authors and especially Kendall (1981) showed that the boundary layer just beyond the roughness peaks follows displaced Blasius profiles, i.e. is governed by molecular rather than eddy transport. The plausible inference from the total evidence suggests that the low-inertia flow regions below the roughness peaks modifies substantially the receptivity to external disturbances from that of a smooth wall. When the TS wavelengths exceed 15-20 times the characteristic roughness scale, the crucial y and x phasing of TS waves evidently remains unimpaired. These inferences should be verified by controlled experiments designed for the specific testing of the mechanisms.

The preceding roughness role in transition is distinct from the larger roughness role covered on the right side of Fig 11, and was not previously suspected. The third technologically all-important roughness role on the roads to turbulence is that of very small distributed roughness. This is probably not a receptivity problem: at such low Reynolds numbers, the roughness generates steady vorticity, especially  $\omega_x$ . Any unsteadiness must be associated with an instability forced by a "cooperating" disturbance agent, such as freestream turbulence. Conceptually, the small-roughness effect remains an irritating bypass, almost an insult to our engineering soul.

## 5. CHAOS AND TURBULENCE IN OPEN-FLOW SHEAR LAYERS

### (5.1) Instabilities, forcing disturbances, receptivities and chaos prediction

In Section 2, we outlined the observed development of sequences of instabilities and onset of turbulence in x-dependent open-flow systems. In Section 3, we established that except in the infrequent cases of global instability, environmental disturbances (not the intrinsic properties of the initial shear layer) control the instability sequences on the road to turbulence, and dominate the irregular character of vortical structures. Thus in this vast class of technologically important flows the concepts of chaos and strange attractors offer little if any help with the design task of predicting transition.

Since, as explained in Section 4.5 in conjunction with Fig 10 we cannot expect to have adequate information about the environmental disturbances - the input into the instabilities - we must establish rational bracketing estimates in spite of these uncertainties and a matching philosophy of risk in design; see Morkovin (1978) for further discussion. For the purposes of the present review, only the rationally solvable aspect of the problem of receptivity paths for the external disturbances were taken up in Section 4. That completes the account of the main recent conceptual and physical advances in understanding transition to turbulence in open-flow systems.

In the Appendix, we provided the essential descriptive background for the conceptually and philosophically important notion of chaotic behavior. We can now return to the questions posed in Section 2.5 concerning the relation of chaos, transition to turbulence and turbulence in open-flow systems. In Sections 5.2-5.4 we shall reexamine three flows (one of them globally unstable) to set the stage - for more questions. Currently the uncertainties and irregularities of the subject in open-flow systems lead naturally to questions and few answers if any. However, with the recent clarification of concepts of

convective and global instabilities, the questions should be sharpened. In fact, an experimenter should well consider the various questions in Section 5.2-5.5 and Fig 13 and 14 before embarking upon the time-consuming search for chaotic characteristics in open-flow shear layers.

(5.2) The case of a chaotic laminar slender wake

The beautiful visualization of Fig 12 of Stuber and Gharib (1988) display for us four modes of behavior of a slender wake downstream of a 63A008 airfoil under various intentional excitations by local wall heating in water. These should help to make the concepts in the Appendix and Fig A-1 more concrete - and raise some more general questions stimulated by the behavior of this specific fluid oscillator.

The slender wake is convectively unstable so that it responds to a band of frequencies which widens with excitation level (though the band is much narrower than that of mixing layers). Subject to the indigenous environmental disturbances the spectrum at the primary probe position 3 chord lengths downstream shows a broad-band hump between 2.2 and 5.8 Hz, with most energy between 4 and 4.6 Hz. This is in sharp contrast to the globally unstable bluff wakes and mechanically rigid oscillators, where the oscillations are very regular. Nevertheless the investigators identify 4.075 Hz as the "natural" frequency  $f_n$  and study the properties of this nonlinear Navier-Stokes system with rather strong forcing, as seen in Figs 12a-c.

The forcing at  $f_n$  in Fig 12a makes the oscillator more regular: the excitation overrides the competing frequencies in the convective instability and reduces the background broadband spectrum by factors roughly from 10 to 50. The quasiperiodic  $f_1$  and  $f_2$  forcing of Fig 12b should place the system on the torus of the 3 phase space in Fig A-1c, although spectra in Fig 7 of Stuber and Gharib (1988) indicate that the oscillations are more complex. Evidently the convective instability elicits more degrees of freedom in the open-flow environment.

In accordance with Section A-3, forcing by the three frequencies in Fig 12c should make the wake chaotic (as the spectra seem to confirm). However, according to Stuber and Gharib (1988) examination of more extensive visualization records disclosed "some areas of strong mixing". Since in Fig 12c no local fuzziness nor obliteration of streaklines (Section 2.5) is evident, the original label of "laminar" was retained for this specific realization. In principle, twodimensional laminar chaos should be possible and may presumably correspond to so-called twodimensional turbulences (Section A-4). If at this speed the local turbulent mixing is sporadically present, a reduction in Reynolds number would probably produce a true laminar though not necessarily twodimensional chaos.

Sporadic local onset of turbulence is common in bluff wakes. In fact, its march upstream towards the body with increasing Reynolds number modifies the wake characteristics significantly, Fig 13, top. Such localized onsets of turbulence in a sea of laminarity bring out a basic question: how does one usefully characterize the state of a shear layer in the theory of dynamical systems when it displays laminarity and turbulence side by side? See also item (2) on the right of Fig 14.

The visualization in Fig 12d was carried out by K. Stuber at the author's request. The turbulent structures are "natural" in the sense that no oscillatory forcing was applied in this case. The boundary layer was turbulent at the trailing edge of the airfoil. The fuzziness of the lines testifies to small-scale turbulent diffusion which is not present in the other visualizations. The intent was to suggest that turbulence and chaos are not synonymous in open-flow systems. Paradoxically, the same conclusion was reached recently by Heslot, Castaing, and Libchaber (1987) in their experimental study of a Bénard-Rayleigh cell - a closed-flow system! Further discussion of this issue will be taken up at the end of Section 5.5.

The paper of Stuber and Gharib also illustrates the nature and the approximate validity of temporal phase-space reconstruction and

Poincaré sections for the cases of Fig 12a-c. However, the determination of Lyapunov exponents (Section A-3) in their Fig 17 shows them to be positive for the non-chaotic states of Fig 12a and b. This is a significant conceptual discrepancy which they "attribute to noise inherent in an open system". Clearly the value of the concepts of chaos deteriorates unless rigorous procedures can be established for separating the intrinsic chaotic features from extrinsically driven random features in the flow response; see item (3) on left of Fig 14.

All the measurements were taken at a single point or single x station. How well can such measurements characterize the properties of the whole system, especially in an x-developing shear layer? (Item (2) on left of Fig 1.) Admittedly, Deissler's reasoned call for measurements of Lyapunov's exponents in a convective frame of reference, Section A-4, is difficult to carry out experimentally. However, the "optimal space-time correlations" of Favre et al (1953) substantiate Deissler's criticism. Since they take into account the convection of large structures they may lead to improved procedures: see Question Q<sub>2</sub> in Fig 14 and Section 5.5.

The preceding questions sparked by the Stuber-Gharib experiment do not imply any criticism of the experiments. After all their intent was to "test the waters" for the applicability of the new concepts and procedures in a relatively simple and controllable open-flow system. They accomplished their purpose well. The author is grateful for their help with Fig 12 and for an early manuscript, which helped to broaden the range of the planned general questions.

### (5.3) Road to turbulence in a globally unstable flow

In view of the central role of convective instability in forcing and controlling the sequence of instabilities on the road to turbulence, it is instructive to examine the major features of a similar evolution as Reynolds number increases in an unidealized globally unstable open-flow system, namely that downstream of circular cylinders, upper part of Fig 13. Both the globally unstable near wake as well as the



local incipient turbulent spots at some Reynolds numbers. Therefore, the two questions at the top of Fig 13 are in order in the context of Section 5.

In a globally unstable near wake vortical structures are still convected away without the chaos-generating iterative recycling present in closed-flow systems. However, part of their unsteady signature is conveyed upstream and thereby helps to create a partially closed system with respect to temporal disturbances. Thus open-flow globally unstable systems have one important feature in common with closed-flow systems. The applicability of chaos concepts may therefore be more likely in globally unstable cases than in the convectively unstable ones.

Sections 3.2 and 3.4 established the basis for the global instability of near wakes and described the temporal evolution to the final saturated x-resonant flow field. Measurements by Nishioka and Sato (1978) and Unal and Rockwell (1988) in this final field disclose a spatial exponential growth in x of the harmonic oscillations  $u'$ . The strict global-instability regime extends only between (aspect-ratio dependent) Reynolds numbers of 45 and 160, with two minor puzzles, still unresolved. The "clockwork oscillatory regularity" of Roshko (1955) is interrupted by small discontinuities near  $Re$  of 90-100, apparently associated with a change of shedding pattern and possible threedimensionality, see discordant accounts of Tritton (1959), Gaster (1971) Berger and Wille (1972), Gerrard (1978) and Friehe (1980). Furthermore, in some low- $Re$  experiments, the phase of the vorticity varies linearly along the span yielding swept-back vortices.

Smaller-scale spanwise nonuniformities appear near  $Re$  of 200. Gerrard's (1978) visualizations suggest the presence of vorticity feedback to the separation line - as postulated in absolute instability - for this spanwise threedimensionality, Fig 13. At about the same Reynolds number local regions of high diffusivity (incipient turbulence spots of Section 2.5) appear at first quite far downstream in the convective-instability domain. Also at about the same  $Re$ , a startling

change in the nonlinear upstream influence takes place: a reversal in the Re-trend of base pressure and oscillatory lift coefficient on the cylinder (both of technological importance); see introduction in Unal and Rockwell (1988). These trends reverse again for  $Re > 2000-10,000$  (depending on aspect ratio).

Despite various conjectures, Gerrard (1978), Unal and Rockwell (1988), no convincing explanation has yet emerged for either reversal. A correlating scale seems to be provided by the formation length of Gerrard,  $l_F$  sketched in Fig 13. This length corresponds to the crossing of the centerline by the rolling-up vorticity sheet when the first vortex is shed. The system, which now includes threedimensional vorticity, evidently remains globally unstable. The cause of the reversals must therefore be sought in the changes of the vorticity distributions and (possibly competing) instability modes in the immediate near wake as Re increases. Symmetric Gerrard-Bloor instability (which at higher Re is associated with the thin individual separating layers rather than with D) and the aforementioned smaller-scale spanwise threedimensional instability could well interfere with the basic Karman-Bénard mode. The simple global instability model probably will not be able to account for the subtle changes in these vorticity fields and their multiple instabilities as Re increases. Nor can one expect chaos theory to unravel the puzzle in this highly x-dependent shear layer.

With growth in Re comes also the upstream march of the first onset of turbulence  $Tu$ , Fig 13. We could expect changes in behavior when  $Tu$  first reaches the boundary between global and convective instability or the fluid in the first shedding vortex. These conditions probably modify but do not destroy the global instability of the main oscillator, but the author is unaware of any studies of such effects. The Gerrard-Bloor vortices increase in frequency and become smaller. At higher Re many of them crowd into the shear-layer segment which rolls up into the first large vortex at  $l_F$ . The first bursts of turbulence then apparently become associated with higher instabilities of the strained unsteady Gerrard-Bloor vortices. They ultimately reach

the proximity of the oscillating separation line on the cylinder.

It has been recognized only in the Fifties that the subsequent classical rapid decrease in drag takes place through the formation of laminar bubbles when the oscillating free turbulence shear layer reattaches to the cylinder. This terminates any global instability features in the near wake of circular cylinders. The reattachment process is random in space and time and very sensitive to freestream disturbances (especially in  $\omega_x$ ) because the instability in the individual separated layers is convective. The entrainment effects within the bubbles are commonly uneven with consequent asymmetry of the mean flow. The rest of the listings in Fig 13 for still higher Reynolds numbers are also technologically important. However they relate now to convectively unstable boundary layers under high acceleration and are included here merely for the sake of completeness.

It seems clear that despite the important feature of global instability, the prospects of clarifying any of the significant details of these high-Re phenomena in an open-system with strong x-dependence through concepts of chaos are virtually nil. To be fair no such claims have been made for this specific applicability, as they have for the power of modern computers. It seems safe to repeat after 24 years, Morkovin (1964), the opinion that these too are unlikely to handle the important threedimensional and locally turbulent features of the flows described in Fig 13 for quite some time.

It is worth remarking that much of the complexity of these flows is associated with the interplay between the unsteady, variable, often spanwise nonuniform, separation line and the nonlinear pressure gradients. In bluff flat-based wakes such as that of Hannemann and Oertel (1988), where the separation line is fixed at the straight shoulders global instability persists when the separating boundary layer becomes turbulent! If its thickness is small with respect to the base height, the high-frequency small-scale turbulence at separation has remarkably little influence on the wake oscillator including its frequency.

(5.4) Road to turbulence in a boundary layer:  $e^N$  method

The cases examined in Sections 5.2 and 5.3 had inflectional instability. In contrast the primary instability in the boundary-layer evolution depicted in the lower half of Fig 13 is viscosity induced. Nevertheless, it is convectively unstable as was the slender wake of Section 5.2 so that many comments and questions need not be repeated. Since excitation by unsteady pressure gradients was covered in Section 4.6, the response selected here for examination is that to low freestream turbulence.

Despite Kendall's misgivings cited in Section 4.7 we assume that coherent freestream structures, strained and accelerated by the body pressure field enter the boundary layer or pass near it and induce laminar TS spots as mandated by satisfaction of all the boundary conditions, left side of Fig 11. In accordance with the character of convective instability Fig 5a, these spots grow while propagating downstream; they merge and superpose. A hot wire would measure modulated, slightly shifting frequencies of an x-amplifying u fluctuation. Since 2D waves are generally more amplified than skew waves, the averaged response would appear close to a quasitwodimensional growth in x.

The sequence of 3D secondary instability, tertiary instability, and intermittent onset of incipient turbulent spots between  $Re_{tr-beg}$  and  $Re_{tr-end}$ , sketched in Fig 13 summarizes the material discussed throughout Section 2. The label under the primary instability emphasizes the fact that the amplification rate of TS growth is slow and that the sketch distorts the x scales to accommodate the explanations. In reality the x-range between  $Re_{cr}$  and the beginning of the secondary instability vastly exceeds the combined x-range of the secondary and tertiary instabilities.

A.M.O. Smith (1956) and Van Ingen (1956) suggested independently that this evident primary control of the transition process by the

involving TS instability. With the blossoming of computer technology this technique based on the ratio of linearized amplification between  $Re_{cr}(f)$  for any frequency  $f$  and any station  $x$ ,  $e^{N(x)}$ , has been widely applied and extended, e.g. Bushnell, Malik and Harvey (1988). The following comments on judicious use of the technique are appropriate in the spirit of Section 5.

The crucial choice of  $N$  (say from 5 to 12 in free flight) clearly depends on estimated environmental disturbances for all convectively unstable shear layers. Philosophically, the risk to the design objectives and the possibility of bypass transition, Fig 15, in uncharted flow fields (including wall roughness generation in superhot hypersonic environments) should be accounted for. The very term "prediction" instead of "estimation" indicates a tendency to an optimistic overbelief by engineers: we tend to endow the results of our simplified computer codes for idealized flow fields with an unwarranted aura of reality.

The basis for inferring the quality of "controlling slow-rate amplification" for primary instabilities other than the low-speed TS instability needs buttressing. The reliability of computer codes for calculating accurately enough subtle boundary layer profiles and the corresponding  $Re_{cr}(f)$  and amplification rates, integrated over the path of the laminar spots (e.g. for 3D boundary layers with wall curvature, hypersonic boundary layers, etc.) is largely untested. The critical "semiempirical" choice of  $N$  for any class of flows is a subjective process of judgments across several disciplines. It involves judgments across the Mach number and Reynolds number range on specific linear instability theories, on specific computer codes, on the onset of transition in the few experiments with sufficient detail information, on the quality of environmental disturbances in these experiments, etc.

Such judgments have come largely from a single group at NASA Langley Research Center. As a friend and an old industrial hand at transition estimates, the author is supportive of the objectives and efforts of the group. Nevertheless, it is appropriate to quote here the modified Guideline No 4 of the U.S. Transition Study Group,

Reshotko (1976). "Whenever possible, tests and numerical computations should involve more than one facility. Tests and computations should have ranges of overlapping parameters, and whenever possible, experiments should have redundancy in transition measurements and transition-estimating personnel." The issues here transcend the narrow professional questions about which author is more correct in what paper. In view of the magnitude of private and public funding involved, these are national issues.

Figure 13, bottom also cautions us about the so-called unit-Re effect. Whenever freestream velocity or stagnation pressure is changed transition on the model changes not only in  $x$  but also in the dimensionless parameter  $Re_{tr}$ ! This pernicious nonconstancy of  $Re_{tr}$  is usually conveyed in plots of  $Re_{tr}$  vs  $Re$  per unit length,  $Re_L$ ; hence the misleading name. The diverse variations merely indicate that for any model in any facility there are more than one characteristic length or velocity which influence palpably the transition process. There is no single unit-Re effect! Notorious contributors to these variations come from leading-edge geometries, roughness and freestream disturbances, including sound radiated from turbulent sidewalls in supersonic wind tunnels. The unit-Re effects make it difficult to compare transition results between facilities and free flight and complicate the life of transition estimators.

The comment on the right of the sketch raises an untackled issue for research in turbulent boundary layers: to what extent do the properties studied in a given realization reflect generic intrinsic turbulent-layer characteristics, uncontaminated by the nonuniformities in the preceding laminar layer including the extensive transition region? The question is relevant whether the transition occurs "naturally" or is artificially induced.

(5.5) On experiments on chaos in open-flow systems

The account of observed real-life routes to turbulence in the three classes of flows in Sections 5.2-5.4 prepared us for further discussion of the questions posed in Section 2.5. The central questions concern the manner in which the successive phenomena in the sketches of Fig 13, could be related to dynamical states, including chaos: the definition of the state of the system (see Section 5.2) and the existence of a strange attractor associated with each segment of a shear layer which grows with  $x$ . The relative success of the linear instability theories rests on the fact that linear instability characteristics, especially the amplification rate, are almost-local properties of each segment of the shear layer. We can define the functional dependence  $\alpha_i(x)$  and use it in our computations. Can a strange attractor be related to each segment of a chaotic or turbulent layer growing in  $x$  by a specific rigorous procedure? If not, repetition of techniques taken over from experiments on closed-flow systems, would be illusory with superficial, if any meaning.

The notion that a major difference between open and closed systems lies in the fact that vorticity structures in the former are convected away and not recycled as in the latter was brought up in Sections A-4 and 5.2; see also the contrast between statements (a) vis-á-vis (b) and (c) in Fig 14. Deissler (1985) in effect states that the divergence properties characterized by Lyapunov's exponents are not "almost-local" and that a convective framework is needed to elicit them in his "simple" equation (i.e. with coefficients not explicitly dependent on  $x$ ). Are other properties, such as the Strange Attractor S.A., itself and its dimensions also attached to the traveling vorticity structures?

If that were so for Deissler's model, determination of these properties would become questionable in all open-flows where the shear layers changes in  $x$ . The asymptotic target would be constantly changing so that for practical purposes the properties would be undefinable; see contrast in statements (1) on both sides of Fig 14. Modernized spatio-temporal multiple-probe techniques of Favre and

coworkers,  $Q_2$  at bottom of Fig 14, might possibly characterize the intrinsic properties in constant-scale turbulent flows such as those in pipes. That would appear to be a meaningful but difficult experiment which should clarify the convective aspects of any chaotic properties. The studies of Wygnanski and Champaign (1973) of turbulent puffs and slugs provide support for this notion.

Even pipe flows, Fig 1b, contain segments of x-dependent internal boundary layer growth which make them at least locally convectively unstable. As such, pipe flows may be imprinted by extrinsic noise before they become fully turbulent. As in the case of the boundary layer at the end of Section 5.4, the question arises whether the fully turbulent structures in pipes have any memory of their noise-controlled past or how rapid the memory loss may be. This is related to the question of separation of intrinsic chaotic features from externally driven random features; see items (3) in Fig 14 and discussion of noise at the end of Section A-4. The turbulent pipe-flow experiment in the preceding paragraph could then be usefully followed up with studies of effects of diverse intentional disturbances which trigger different upstream transition patterns.

Figure 14 summarizes the various issues which distinguish between concepts and their experimental verification in closed-flow and open-flow systems. The preceding discussion justifies the label "controversial" on top right of Fig 14, and the skepticism with respect to single-point measurements, especially in open-flow systems. What substantive information can be inferred from a time trace at a single point of a growing turbulent shear layer? Only multiple-point multiple-probe information can help to clarify the modifications brought about by the uniterated convection of vortical structures.

As noted in Section 5.2, the one experiment in the literature reporting two-point measurements is for a closed (!) Benard-Rayleigh cell, heated from below (in which buoyancy-driven vorticity recirculates in place). The results created considerable commotion: Heslot, Castaing, and Libchaber (1987) confirmed that chaos and turbulence are



not synonymous. As the Rayleigh number increased they observed "the onset of the oscillatory instability followed by the now well-known routes to chaos", specifically through a period-doubling cascade proposed theoretically by Feigenbaum. The correlation dimension of the temporally chaotic state varied from  $2 \pm 0.1$  to 4, before the coherence between the bolometer at half height of the cell and the bolometer near the bottom wall started decreasing from nearly unity for all significant frequencies to a negligible value. The loss of coherence and the disappearance of the identifiable chaotic state was attributed to the formation of a boundary layer at the wall.

As the Raleigh number was pushed higher and higher they observed two extended regimes of "soft" and "hard" turbulence. The first, with very little coherence between the two bolometers, is interpreted in terms of unsteady rolls with locally detached laminar boundary layers and random phasing, a state called phase turbulence in some quarters. The hard turbulent state is interpreted in terms of a turbulent boundary layer at the base with abrupt detachment of thermal flumes which reestablish communication and coherence between the two bolometers (one above the other). Interestingly, the interpretations are supported by dimensional arguments from engineering turbulent boundary layer theory, besides spectra, timetraces, probability density, etc. In other words, even in closed systems, we ultimately have boundary-layer formation, detached shear layers, etc. and need to speak of them as distinct entities, with turbulence on their local scales, as in Section 2.5.

In the authors' language: "we have in some ways brought together the two approaches to turbulence. The dynamical system approach is a very good analysis of the onset of (temporal) disorder, as one slowly increases the Rayleigh number...It is followed by a state where space disorder sets in. In this regime, the development of a boundary layer, laminar at first and later turbulent, leads to two distinct turbulent states..."

Chaos concepts are evidently of little help after the spatial disorder commences. Can the chaos concepts be at least conceptually fruitful in open-flow shear layers, where we begin with already formed boundary layers? How much is their significance weakened by the downstream convection of vortical structures absent in the Benard-Rayleigh experiments. And by the growth in the layer thickness? Some of the suggestions in this section concerning experiments may help to provide at least partial answers.

## 6. CONCLUSIONS

Roads to turbulence in open-flow systems can be interpreted fruitfully as sequences of often competing instabilities corresponding to primary and higher-order restructuring of vorticity distributions; see summary Figures 2, 3, 13 and 15. The recently clarified concepts of convective instability and global instability unify previously fragmentary observations of fluctuation behavior, Section 3. In particular, a large majority of technologically important open-flow shear layers, which belong to the convectively unstable families, are unquestionably driven by ever-present small environmental disturbances. Consequently in these flows, concepts of chaos and strange attractors (introduced in the Appendix) offer no help with prediction of transition to turbulence.

To help understand forcing by external disturbances the disturbances are first classified into families with different propagation characteristics, Fig 10. These disturbances are first strained or diffracted by the wall geometry of tunnels and models. Depending on their propagation characteristics and the straining near and in the shear layer, these external disturbances are converted into internal unstable modes of Tollmien-Schlichting-Schubauer, Goertler, and cross-flow primary vorticity restructuring and into more complex modes of secondary and higher instabilities. The process of conversion was identified by the author in 1969 and called receptivity. Several types of receptivity paths are demonstrated by experiments selected from recent literature, Figs. 8 and 9 and Sections 4.3-4.6. When the external disturbances are small, the forcing corresponds to a nonhomogeneous linear problem, which is solvable in principle, Fig. 11. The mathematical and physical basis of several receptivities is outlined.

Receptivity analyses should alert us to the most dangerous receptivity paths for any given configuration. They will not help with direct estimates of transition because the disturbance flow fields will not be known a priori in wind tunnels or in flight. Because of the large total amplification of the disturbances, the initial forcing fields are too weak for adequate diagnostics and

measurements of the distinct families of disturbances of Fig. 10. Since the input into the various instabilities will remain uncertain we have to resort to engineering estimates and bracketing with the powerful but tricky aid of computers. The philosophy of approach to such estimates, in particular, the  $e^N$  method, is examined in Section

5.4 In Section 5 we return to the questions posed in Section 2.5: To what extent are the classical turbulent states in open-flow systems equivalent to chaotic states? What deeper insights can the theories of chaos bring to our dealing with turbulence in open-flow systems? The attempts at answers raise new questions about the effects of vorticity convection and of x-dependence of the shear layers on the nature and existence of strange attractors in open flow systems - see Fig. 14. The roads to turbulence in three real-life shear layers, (one with the partially closed system of disturbances rather than of mass and vorticity) are examined for clues in Sections 5.2-5.4. Doubts arise about the meaning of single-point measurements taken over from experiments in closed-flow systems. Modernized multiple-probe optimal space-time techniques of Favre and co-workers are suggested to help to answer the vorticity-convection and x-dependence issues.

The new experiments of Stuber and Gharib (1988) in slender wakes and Heslot, Castaing, and Libchaber (1987) in a closed Bénard-Rayleigh cell heated from below suggest that chaos and turbulence are not synonymous. The latter, closed-flow experiment (the only substantial one yet reported using measurements at two points) indicates that chaos concepts are of little help once space disorder as contrasted to temporal chaotic disorder sets in. In this closed-flow, space disorder appears when the controlling parameter is high enough for the formation of boundary layers. In open-flow systems we have boundary layers and separated shear layers as an initial given! Thus current evidence points to negative answers to the two questions about chaos and turbulence.

In summary, the concepts of convective and global instabilities help us to unify diverse observations on instabilities and transition in open-flow systems and confirm the role of environmental

disturbances. The roads to turbulence are physically and theoretically clearer. However, the nature of transition estimation has not changed; only the perspective and the tools have improved.

At this stage of developments the concepts of chaos and strange attractors show little if any promise in this task. The name of our technological game is "convected spatial disorder in x-growing shear layers" not "temporal disorder in recycled closed systems of constant scale". Transition and turbulence in open-flow systems are evolutionary processes, not balanced, equilibrated states. The serious difficulties in applying these concepts to high-Re open flows should not detract from their great conceptual and philosophical significance in less complex, more cohesive nonlinear systems across scientific disciplines.

It is impossible to trace the myriad of discussions, letters and papers which have influenced the perspective offered in this review. To all those contributors the author is grateful for keeping him curious and young in retirement. Many are acknowledged indirectly by citation of their papers. The author also wishes to acknowledge partial financial support in preparation of this review under AFOSR Grant No. 86-0165 and a grant from ICASE and the Computational Methods Branch of NASA Langley Research Center.

APPENDIX: A TASTE OF CHAOTIC BEHAVIOR

(A-1) New concepts and philosophical implications

Chaos theory uses language far removed from engineering terminology. The most accessible exposition of the field is found in the books of F.C. Moon (1987) and Bergé, Pomeau and Vidal (1986). Here we propose merely to illustrate how a nonlinear Van der Pol oscillator can undergo chaotic motion in response to pure harmonic forcing, a behavior seldom discussed in engineering courses. The abstractions of chaos may not impact practical engineering concerns in turbulent systems for a long time. Conceptually, however, they provide a new basic insight: erratic or chaotic behavior is to be expected across disciplines in DETERMINISTIC nonlinear systems with just a few degrees of freedom even in absence of random disturbances.

Turbulence was discovered more than a century ago and fluids engineers have known over forty years that its onset occurs after just a few instabilities. The recognition that qualitatively similar aperiodic behavior takes place commonly in sufficiently nonlinear mechanical (e.g. vibrations), electrical, biological, chemical, ecological, etc systems provides a unifying philosophical perspective on our world. That fibrillation in the human heart heralds the onset of a chaotic mode of this electromechanical system represented a revelation which in turn helped the design of defibrillators. Darwin too would have found the concepts of chaos stimulating.

(A-2) Limit cycle - attractor

The Van der Pol oscillator mimics flow instabilities in allowing small displacements  $y$  at small velocities  $\dot{y}$  draw energy from the system and grow by virtue of the locally negative damping coefficient  $\epsilon(y^2-1)$  of  $\dot{y}$  in the equation shown in Fig A-1. In the unforced case

(1),  $b = 0$ , the motion is thus self-excited. For this second-order system, we need to specify the initial values of  $y$  and  $\dot{y}$  (termed phase or state variables) to evaluate the constants of integration and obtain a specific solution in time. As Fig A-1b shows, an initially small displacement amplifies rapidly for the parameter value  $\epsilon = 1$  before it "saturates" at a fixed amplitude. In an autonomous system (one without explicit time dependence in the equations) it is possible to express one phase variable in terms of the others at all times and plot them against each other, as in Fig A-1a for the 2-phase space.

The specific time-trace solution of Fig A-1b corresponds to the inner trajectory, unwinding from the origin in Fig A-1a toward the saturation curve C, called the limit cycle. For any initial state of the oscillator, i.e. any point  $y(0)$ ,  $\dot{y}(0)$  within the contour C, there is a unique inner trajectory through this point. Each solution-trajectory unwinds towards larger  $y$  and  $\dot{y}$  values and approaches C asymptotically. An infinity of these trajectories corresponding to all initial state variables inside the contour, crowds outward toward C from within. Solutions associated with initial  $y(0)$ ,  $\dot{y}(0)$  values outside of C have positive damping, lose energy and wind down towards C, the common asymptote. Only two are shown in Fig A-1a, but again there is an infinity of these outer trajectories crowding down towards C. Given the  $y$  dependence of the damping, the geometry and direction of the trajectories is set. In a 2-phase space the long-time solution-trajectories are thus constrained to approach a single finite-amplitude closed curve, the periodic limit cycle, the dominant intrinsic characteristic of the nonlinear oscillator. These long-time solutions are insensitive to initial conditions. The Karman-Bénard vortex street close behind a cylinder for  $45 < Re < 160$  exemplifies such a periodic attractor in an open-flow system.

### (A-3) Oscillator forcing - threedimensional phase space

When the Van de Pol oscillator is forced harmonically, the term  $\epsilon b \omega \cos \omega t$  on the right side of the equation in Fig A-1 renders the system non-autonomous. To obtain solutions-trajectories with properties similar to those in the 2-phase space of Fig A-1a, we

eliminate the explicit  $t$ -dependence of  $\cos\omega t$  by introducing a third phase space variable through  $\dot{\theta} = \omega$ . The forcing term becomes  $\cos\theta$  as can be seen in the equivalent set of three first-order equations in Fig A-1. Again, for any combination of the parameters  $\epsilon$ ,  $b$  and  $\omega$ , there is a unique trajectory-solution through every point of the 3-phase space determined by the prescribed initial values  $x$ ,  $y$ , and  $\theta$  at  $t = 0$ .

For some parameter combinations, as the transients subside the solutions are asymptotically attracted to the toroidal surface in Fig A-1c, the generalization of the one-dimensional limit cycle. The quasiperiodic laminar wake oscillations in Fig 12b correspond to such an attractor with two noncommensurate frequencies  $f_1$  and  $f_2$ ; see Stuber and Gharib (1988) for more details.

For some parameter combinations, however, the trajectories become disorderly, as if drunk with the freedom of motion provided by the extra phase dimension. The contorted family of trajectories still fills the 3 space, but is locally more dense in some regions, as it was in the proximity of the limit curve  $C$  in Fig A-1b. As time increases indefinitely the transients die out and the trajectories approach an attractor subspace not describable in terms of classical geometry. This "strange attractor" is made of an infinite discrete set of convoluted, nearly parallel surfaces with spacing becoming locally infinitesimal.

The asymptotic set does not fill the 3 space completely; nor is it a finite sum of two-dimensional surfaces. The attractor has an effective fractional dimension between 2 and 3. Various determinations of the "fractal dimension" of a strange attractor naturally require limiting procedures and large amounts of numerical or empirical data, with attendant problems in accuracy, Moon (1987). Yet the attractor dimension is a quantitative intrinsic property of the given nonlinear system which distinguishes it from other systems. A fluid system governed by Navier-Stokes equations could potentially have very large dimensions so that some critics question inferences of behavior based on experiences with low-dimensional systems. Sreenivasan (1985) estimated dimensions on the order of 20 in a cylinder wake at Reynolds



numbers near 10,000.

In forced chaotic systems, sampling of the state variables at discrete periods  $2\pi n/\omega$  corresponds to so called Poincaré sections labeled P in Fig A-1c through which one can study the evolution of the system in more detail. In this figure the signature of the quasiperiodic regime i.e. intersections of the asymptotic trajectories with the Poincare cut, are seen to aggregate into the closed curve Q. For the chaotic regime, Figure 3-14 of Moon (1987) shows the intersections of the asymptotic trajectories to form an infinite set of "highly organized points arranged in what appear to be contorted parallel lines". When one enlarges a portion of the section, similar, smaller-scale structure is revealed, a characteristic of fractal sets. This phase-space structure is reflected in the aperiodicity of time traces of any state variable and their broad-band spectra. An oscillator, driven sinusoidally at constant frequency may respond in gibberish, not noise-induced, but deterministic gibberish! The Duffing oscillator, with linear positive damping and a cubic spring element responds similarly.

The equations are relatively simple; even the crucial nonlinearity in the Duffing case is simple. Yet predictability and reconstruction of the past is thwarted. In principle, the results are repeatable. But there exists extreme sensitivity to initial conditions which control the specific solution-trajectory. Neighboring trajectories in chaotic systems tend to diverge exponentially in time, the divergence being characterized by positive Lyapunov exponents - another "measurable" property of the system. A minute change in the initial value, say of the velocity  $\dot{y}$ , may therefore cause a shift to a different region of the attractor and different asymptotic gibberish.

#### (A-4) On implications for open-flow systems

The nonlinear behavior of systems with two and three degrees of freedom, summarized in Fig A-1, departs significantly from that stressed in undergraduate engineering texts. On one hand there is the

powerful constraint of the limit cycle and toroidal attractors with their lock-in, threshold, jump and hysteresis phenomena, elements of which are evident in all fluid oscillators. On the other hand, there is the intrinsic chaotic behavior which may be a low-dimensional manifestation of phenomena somehow related to turbulence in the high-dimensional Navier-Stokes flows. We first note that Fig 12c demonstrates the existence of chaotic wake motion without threedimensional turbulence. If the motion in that laminar wake could be maintained twodimensional, it would be difficult to distinguish it from theoretical twodimensional turbulence (with possible inverse cascade processes) - if a distinction does exist. Such a twodimensional chaotic flow would be a realization of a Navier-Stokes solution satisfying the turbulent syndromes of Fig 3 except that vorticity would remain twodimensional. The solution would be determined by vorticity dynamics without the powerful tilt-and-stretch mechanism of threedimensional turbulence. The common turbulent wake of Fig 12d would presumably have a different, higher-dimensional attractor. But how to translate the attractor characterization into information in the physical space, of general or specific engineering interest such as entrainment and mixing in the two wakes above? By building up a dictionary of strange attractors?

A major problem is that the theory of dynamical systems has concentrated on evolution in time, and by virtue of its tools has nothing to say about the structure of chaotic flow systems in the physical space. The paradigm is one of temporal chaos. Yet in shear-flow turbulence threedimensional spatiotemporal organization determines the varied transport properties which are of primary interest in engineering. The limited experimental confirmation of chaos theories in flows, Guckenheimer (1986), comes from closed-flow systems: flows between rotating cylinders and the Bénard-Rayleigh layers heated from below. In both, the vorticity is recirculated upon itself ("working upon itself"). Streamwise change of scale and streamwise convection of vortical structures do not play a role as in open-flow systems.

In important open-flow systems vortical structures move downstream while gradually spreading across streamlines. Besides this parabolic behavior in the mean, there generally exists streamwise nonhomogeneity and associated intermittency in the structures comparable to the shear layer in scale. Vortical structures are not recycled; there are no associated iterative processes which are basic to the theoretical generation of strange attractors. In a Bénard-Rayleigh cell or the fibrillating heart, the same object is interacting iteratively with itself. In open flows the objects are passing by. Consequently, if strange attractors can be defined for x-dependent systems, they are likely to be glimpsed by an observer traveling with the objects.

R.J. Deissler (1985) concluded on the basis of numerical experiments with the nonlinear Ginzburg-Landau partial differential equations in  $x$  and  $t$  with a convective term,  $U\partial A/\partial x$ , that if Lyapunov exponents were to be meaningful, the underlying measurements should be carried out in the frame of reference moving with  $U$ . That measurements by fixed probes in a physical shear layer sense primarily the effect of nonhomogeneities from upstream rather than some intrinsic properties of the vortical entities has been recognized among engineers since Favre and coworkers first measured space-time correlations in turbulent boundary layers in 1953.

An associated issue is that of external noise. Noise in flow systems is omnipresent, broad-band and hard to distinguish from manifestations of an intrinsic strange attractor (except when kept very low). However, noisy fields, nonhomogeneous in  $x$ , can be selectively amplified by open-flow laminar shear layers and can give rise to strong nonlinear fluctuations sensed at any  $x$ , Sections 2 and 3. Furthermore, we have seen in Fig A-1 that external harmonic forcing of sufficient magnitude can actually modify the dimensions of the system and bring about chaos where there had been stable periodic behavior. In open-flow systems small-amplitude noise can thus lead to large randomly modulated fluctuations which can add to and even modify the character of the putative intrinsic strange attractor of the shear layer.

This is not the case in closed flow systems where noise generally adds a low-level broad-band background, except when several modes of incipient instability compete at a critical stage and perhaps in the more erratic cases of large aspect ratios, Guckenheimer (1986). Deissler and Kaneko (1985) mimicked the open-flow noise amplification with the cited Ginsburg-Landau model even without the troublesome  $x$ -dependence of the shear-layer thickness. They conclude that the "noise sustained structures" are both seeded by the noise as well as destabilized by the remaining noisy features after saturation. While the secondary instability in their model is rather specialized (side-band instability) their generalizations agree with our account of primary and secondary instabilities and their inductions in Sections 2 and 3.3.

The issues raised in this Section prepare the discussion in Sections 5.2 - 5.5 where they are further elaborated in context of specific families of flow fields.

## R E F E R E N C E S

- ANDERECK, C. D., LIU, S. S. & SWINNEY, H. L. (1986): Flow regimes in a circular Couette system with independently rotating cylinders, v 164, 155-183.
- ARNAL, D. (1984): Description and prediction of transition in two-dimensional incompressible flow, 2-1 to 2-71, Special Course on Stability and Transition of Laminar Flow, AGARD-R-709.
- ARNAL, D. & JUILLEN, J. C. (1979): Experimental results on the influence of the transition process on the initial structure of the turbulent boundary layer. (In French) ONERA reprint T P No. 1979-128.
- BAYLY, B. J., ORSZAG, S. A. & HERBERT, T. (1988): Instability mechanisms in shear-flow transition, Annual Reviews Fluid Mechanics, v 20, 359-391.
- BECHERT, D. W. (1988): Excitation of instability waves in free shear layers, Part 1. Theory, J. Fluid Mech., v 186, 47-62.
- BECHERT, D. W. & STAHL, B. (1988): Excitation of instability waves in free shear layers, Part 2. Experiments, J. Fluid Mech., v 186, 63-84.
- BENNETT, H. W. (1953): An experimental study of boundary layer transition, Kimberley-Clark Corp. Rept., Neenah, WI, ASTIA Doc. AD18379.
- BERGE, P., POMEAU, Y. & VIDAL, Ch. (1986): Order within Chaos, Wiley & Sons.
- BUSHNELL, D. M., MALIK, M. R. & HARVEY, W. D. (1988): Transition Prediction in external flows via linear stability theory, Proc. IUTAM Sympo. Transsonicum III, Geottingen, Springer Publ. probably 1989.
- CHOMAZ, J. M., HUERRE, P. & REDEKOPP, L. G. (1987): Local and global bifurcations in spatially developing flows, Phys. Rev. Letters, v 60, 25-31.
- CORKE, T. C. (1987): Measurements of resonant phase locking in unstable axisymmetric jets and boundary layers, pp. 37-65 of Nonlinear Wave Interaction, Miksad, Akylas and Herbert, eds., ASME Publ. AMD - vol. 87.
- CORKE, T. C. BAR SEVER, A. & MORKOVIN, M. V. (1986): Experiments on transition enhancement by distributed roughness, Phys. Fluids, v 29, 3199-3213.
- CORKE, T.C., SHAKIB, F. & NAGIB, H. M. (1988): Mode selection and resonant phase locking in unstable axisymmetric jets, submitted for publ. J.F.M.
- DEISSLER, R. J. (1985): Noise-sustained structure, intermittence and the Ginsburg-Landau equation, J. Stat. Physics, v 40, 371-395.
- DEISSLER, R. J. & KANEKO, K. (1987): Velocity-dependent Lyapunov exponents as a measure of chaos for open flow systems Physics Letters A, v 119, 397-402.

- DIMOTAKIS, P. E. & BROWN, G. L. (1976): The mixing layer at high Reynolds number: large-structure dynamics and entrainment, *J. Fluid Mech.*, v 78, 535-550.
- DRUBKA, R. C. (1982): Instabilities in near field of turbulent jets and their dependence on initial conditions and Reynolds number, Ph.D. thesis, Ill. Inst. of Tech., MAE Dept., Chicago, IL 60616.
- FAVRE, A., GAVIGLIO, J. & DUMAS, R. (1953): Spatio-temporal correlations in boundary layers (in French), *Recherche Aeron.* No. 31, p. 37. English versions: *J. Fluid Mech.* (1957), v 2, 313-342 and *J. Fluid Mech.* (1958), v.3, 344-356.
- FIEDLER, H. E. & MENSING, P. (1985): The plane turbulent shear layer with periodic excitation, *J. Fluid Mech.*, v 150, 281-309.
- FLORYAN, J. M. & SARIC, W. S. (1982): Stability of Görtler vortices in boundary layers, *AIAA Jour.*, v 20, 316-324.
- FRIEHE, C. A. (1980): Vortex shedding from cylinders at low Reynolds numbers, *J. Fluid Mech.*, v 100, 237-241.
- GASTER, M. (1971): Vortex shedding from circular cylinders at low Reynolds numbers, *J. Fluid Mech.*, v 46, 749; see also v. 38, 565.
- GASTER, M. & GRANT, I. (1975): An experimental investigation of the formation and development of the wave packet in a laminar boundary layer, *Proc. Roy. Soc. London A.*, v 347, 253-269.
- GATES, E. M. (1980): Observations on transition on some axisymmetric bodies, pp. 351-363 of Laminar-Turbulent Transition, R. Eppler and H. Fasel, editors, Springer Publ.
- GILL, A. E. (1965): A mechanism for instability of plane Couette flow and of Poiseuille flow in a pipe, *J. Fluid Mech.*, v 21, 503-511.
- GINEVSKII, A. S., VLASOV, E. V. & KOLESNIKOV, A. V. (1978): Aeroacoustic Interactions, in Russian. Mashinostroenie, Moscow.
- GOLDSTEIN, M. E. (1986): Proceedings of ICASE/NASA Workshop in Stability of Time-Dependent and Spatially Varying Flows, Springer Publ.
- GUCKENHEIMER, J. (1986): Strange attractors in fluids, another view, *Annual Reviews Fluid Mechanics*, 15-31.
- HALL, P. (1982): Taylor-Goertler vortices in fully developed or boundary-layer flows: linear theory. *J. Fluid Mech.*, v 124, 475-494.
- HALL, P. (1983): The linear development of Goertler vortices in growing boundary layers, *J. Fluid Mech.*, v 130, 41-58.
- HANNEMANN, K. (1988): Numerische Simulation and Stabilitätstheoretische Untersuchung des absolut und konvektiv instabilen Nachlauf. DFVLR-FB 88-09.

- HANNEMANN, K. & OERTEL, H, JR. (1987): Numerical simulation of the absolutely and convectively unstable wake, submitted for publication, J.F.M.
- HERBERT, T. (1988): Secondary instability of boundary layers, Annual Reviews Fluid Mechanics, v 20, 487-526.
- HESLOT, F., CASTAING, B. & LIBCHABER, A. (1987): Transition to turbulence in helium gas, Phys. Review A, v 36, 5870-5873.
- HO, C. M. & HUERRE, P. (1984): Perturbed free shear layers, Annual Review Fluid Mechanics, v 16, 365-424.
- HUERRE, P. (1987): Spatio-temporal instabilities in closed and open flows, pp. 141-177 of Instabilities and Nonequilibrium Structures, E. Tirapegui and D. Villarroel, eds., Reidel Publ. Co.
- HUERRE, P. & MONKEWITZ, P. A. (1985): Absolute and convective instabilities in free shear layers, J. Fluid Mech., v 159, 151-168.
- KALBURGI, V., MANGALAM, S. M. & DAGENHART, J. R. (1988): A comparative study of theoretical methods on Goertler instability, AIAA Paper 88-0407.
- KEGELMAN, J. T. (1982): Experimental studies of boundary-layer transition on a spinning and non-spinning axisymmetric body, Ph.D. thesis, Univ. Notre Dame, IN 46556.
- KEGELMAN, J. T. & MUELLER, T. J. (1986): Experimental studies of spontaneous and forced transition on an axisymmetric body, AIAA Jour., v 24, 397-403.
- KENDALL, J. M. (1981): Laminar boundary layer velocity distortion by surface roughness; effect upon stability, AIAA Paper 81-0915.
- KENDALL, J. M. (1984): Experiments on the generation of Tollmien-Schlichting waves in a flat-plate boundary layer by weak free-stream turbulence, AIAA Paper 84-0011.
- KENDALL, J. M. (1985): Experimental study of disturbances produced in a pre-transitional laminar boundary layer by weak free-stream turbulence. AIAA Paper 85-1695.
- KENDALL, J. M. (1987): Experimental study of laminar boundary layer receptivity to a traveling pressure field. AIAA Paper 87-1257.
- KLEBANOFF, P. S., TIDSTROM, K. D. & SARGENT, L. M. (1962): The three-dimensional nature of boundary-layer instability, J. Fluid mech., v 12, 1-34.
- KOCH, W. (1985): Local instability characteristics and frequency determination of self-excited wake flows. J. Sound and Vib., v. 99, 53-83.
- KOTTKE, V. (1986): Taylor-Goertler vortices and their effect on heat and mass transfer, pp. 1139-1144 of Proc. 8th Inter. Heat Transfer Conference, at San Francisco.

- KOTTKE, V. (1980): A chemical method for flow visualization and determination of local mass transfer, pp. 657-662 of Flow Visualization II, W. Merzkirch, Ed., Hemisphere Publ. Corp.
- KOTTKE, V. & SCHMIDT, K. H. (1985): Measuring Techniques for determination of local mass and heat transfer on industrial scale, pp. 325-335 of Measuring Techniques in Heat and Mass Transfer, Springer Publ., Berlin.
- KOVASZNAY, L. S. G. (1953): Turbulence in supersonic flow, J. Aero. Sci., v 20, 657-668.
- LASHERAS, J. C. & CHOI, H. (1988): Three-dimensional instability of a plane free shear layer: an experimental study of the formation and evolution of streamwise vortices, J. Fluid Mech., v 189, 53-86.
- LAUCHLE, G. C. & GURNEY, G. B. (1984): Laminar boundary-layer transition on a heated underwater body, J. Fluid Mech., v 144, 79-101.
- LAUFER, J. & MONKEWITZ, P. (1980): On turbulent jet flows: a new perspective, AIAA Paper 80-0962.
- LOEHRKE, R. I. & NAGIB, H. M. (1972): Experiments on Management of Free-Stream Turbulence, AGARD Rept. 598, 100 pp., NATO, Paris.
- LOEHRKE, R. I. & NAGIB, H. M. (1976): Control of free-stream turbulence by means of honeycombs: a balance between suppression and generation, J. Fluids Engin., Trans. ASME, v 98, 342-353.
- MACK, L. M. (1984): Boundary-layer linear stability, 3-1 to 3-81, in Special Course on Stability and Transition of Laminar Flow, AGARD Report R-709.
- MACK, L. M. (1985): The wave pattern produced by point source on a rotating disk, AIAA Paper 85-0490.
- MONKEWITZ, P. A. (1988): The absolute and convective nature of instability in two-dimensional wakes at low Reynolds numbers, Phys. Fluids, v 31, 999-1006.
- MONKEWITZ, P. A. & HUERRE, P. (1981): The influence of the velocity ratio on the spatial instability of mixing layers, Phys. Fluids, v 25, 1137-1143.
- MONKEWITZ, P. A. & SOHN, K. D. (1986): Absolute instability in hot jets and their control, AIAA paper No. 86-1882.
- MOON, F. C. (1987): Chaotic Vibrations, Wiley & Sons.
- MORKOVIN, M. V. (1964): Flow around circular cylinder--a kaleidoscope of challenging fluid phenomena, Symposium on Fully Separated Flows, ASME Publ., 102-118.
- MORKOVIN, M. V. (1978): Instability, Transition to Turbulence and Predictability. Keynote address at AGARD Copenhagen Symposium, May 1977, AGARDOGRAPH No. 236, NATO.



- MORKOVIN, M. V. (1983): Understanding transition to turbulence in shear layers - 1983. AFOSR TR-83-0931, AD Number A 134796, available from Nat'l Tech. Info. Service (NTIS), 5285 Port Royal Road, Springfield, VA 22151. Also in AIAA Prof. Study Notes: Instabilities and Transition to Turbulence, with L. Mack, July 1985, Cincinnati, OH.
- MORKOVIN, M. V. (1984): Bypass transition to turbulence and research desiderata, pp. 161-204 of Transition in Turbines, NASA Conf. Publ. 2386.
- MORKOVIN, M. V. & PARANJAPE, S. V. (1971): On acoustic excitation of shear layers, *Zeit. f. Flugwissen*, v 19, 328-335.
- MURPHY, J. D. & RUBESIN, M. W. (1966): A re-evaluation of heat-transfer data obtained in flight tests of heat-sink shielded re-entry vehicles, *Jour. Spacecraft & Rockets*, v 3, 53-60.
- NARASIMHA, R. & SREENIVASAN, K. R. (1979): Relaminarization of Fluid Flows, Advances in Applied Mechanics, v 19, 221-309, Academic press.
- NISHIOKA, M. & MORKOVIN, M. V. (1986): Boundary-layer receptivity to unsteady pressure gradients: experiments and overview, *Jour. Fluid Mech.*, v 171, 219-261.
- NISHIOKA, M. & SATO, H. (1974): Measurements of velocity distributions in the wake of a circular cylinder at low Reynolds numbers, *J. Fluids Mech.*, v 65, 97-112.
- NISHIOKA, M. & SATO, H. (1978): Mechanism of determination of shedding frequency of vortices behind a cylinder at low Reynolds numbers, *J. Fluid Mech.*, v 89, 49-60.
- PIERREHUMBERT, R. T. & WIDNALL, S. E. (1982): The two- and three-dimensional instabilities of a spatially periodic shear layer. *J. Fluid Mech.*, v 114, 59-82.
- PROVENSAL, M., MATHIS, C. & BOYER, L. (1987): Benard-von Karman instability: transient and forced regimes, *J. Fluid Mech.*, v 182, 1-22.
- RESHOTKO, E. (1976): Boundary-layer stability and transition, Annual Rev. Fluid Mech., v 8, 311-350.
- RESHOTKO, E. (1984): Environment and receptivity, Section 4 of Special Course on Stability and Transition of Laminar Flow, R. Michel, ed., AGARD Report 709, NATO, Paris.
- ROCKWELL, D. (1983): Oscillations of impinging shear layers, *AIAA Jour.*, v 21, 645-664.
- ROCKWELL, D. & NAUDASCHER (1979): Self-sustained oscillations of impinging free shear layers, Annual Review Fluid Mech., v 11, 67-94.
- ROSHKO, A. (1955): On the development of turbulent wakes from vortex streets, NACA Rept. 1191 (originally TN 2913, 1953).

- SALWEN, H. & GROSCH, CH. E. (1981): The continuous spectrum of the Orr-Sommerfeld equation, Part 2. Eigenfunction expansions, *J. Fluid Mech.*, v 104, 445-465.
- SCHLICHTING, H. (1979): Boundary Layer Theory, 7th ed. McGraw-Hill Co.
- SHAKIB, F. (1984): Evolution and interaction of instability modes in an axisymmetric jet. M.S. thesis, Ill. Inst. of Tech., MAE Dept., Chicago, IL 60616.
- SREENIVASAN, K. R. (1985): Transition and turbulence in fluid flows and low-dimensional chaos, pp. 41-67 of Frontiers in Fluid Mechanics S. S. Davis and J. Lumley, editors, Springer Publ.
- SREENIVASAN, K. R., STRYKOWSKI, P. J. & OLINGER, D. S. (1987): Hopf bifurcation, Landau equation and vortex shedding behind circular cylinders, pp. 1-13 in ASME Publ. FED-Vol. 52, K. N. Ghia, Ed.
- STERNBERG, J. (1954): The transition from a turbulent to a laminar boundary-layer, Ball. Res. Lab. Rept. 906, Aberdeen Proving Ground, MD.
- STEWART, R. W. (1968): Turbulence, film of Nat. Com. for Fluid Mech. Films; also illustrated summary, pp. 82-88 of Illustrated Experiments in Fluid Mechanics, A. Shapiro, ed., MIT Press, 1972.
- STUBER, K. & GHARIB, M. (1988): Experiments on the forced wake of an airfoil: transition from order to chaos, AIAA Paper No. 88-3531.
- SUTTON, E. P., EVANS, G. P., MCGUINNESS, M. D. & SVEHLA, K. M. (1981): Influence of wall vibration on a flow with boundary-layer separation at a convex edge, 1981 IUTAM Symposium on Unsteady Turbulent Shear Layers, Toulouse. R. Michel, J. Cousteix and R. Houdeville, ed., Springer Verlag.
- SWEARINGEN, J. D. & BLACKWELDER, R. F. (1987): The growth and breakdown of streamwise vortices in the presence of a wall, *J. Fluid Mech.*, v 182, 255-290.
- SWINNEY, H. L. & GOLLUB, J. P. (1986): Characterization of hydrodynamic strange attractors, *Physica* 18D, 448-454.
- TENNEKES, H. & LUMLEY, J. L. (1987): A First Course in Turbulence, MIT Press, 2nd edition.
- THORPE, S. A. (1971): Experiments on the instability of stratified shear flows: miscible fluids, *J. Fluid Mech.*, v 46, 299-319.
- TRITTON, D. J. (1959): The flow past a circular cylinder at low Reynolds numbers, *J. Fluid Mech.*, v 6, pp. 547-567; also v 45, 203-208.
- UNAL, M. F. & ROCKWELL, D. (1988): On vortex formation from a cylinder. Part 1. The initial instability. *J. Fluid Mech.*, v 190, 491-512. Part 2. Control by splitter-plate interference, *ibid*, 513-529.
- VAN INGEN, J. L. (1956): A suggested semi-empirical method for the calculation of the boundary-layer transition region. Report VTH-74, Dept. Aeron. Eng., Univ. of Technology, Delft.

WILKINSON, S. P. &, MALIK, M. R. (1985): Stability experiments in the flow over a rotating disk, AIAA Jour., v 23, 588-595.

WINTER, K. G. & MASKELL, E. C. (1980): The Reynolds number of transition on a flat plate in the RAE 4 ft. x 3 ft. low turbulence wind tunnel, Roy. Aircraft Establishment, Tech. Memo Aero. 1854.

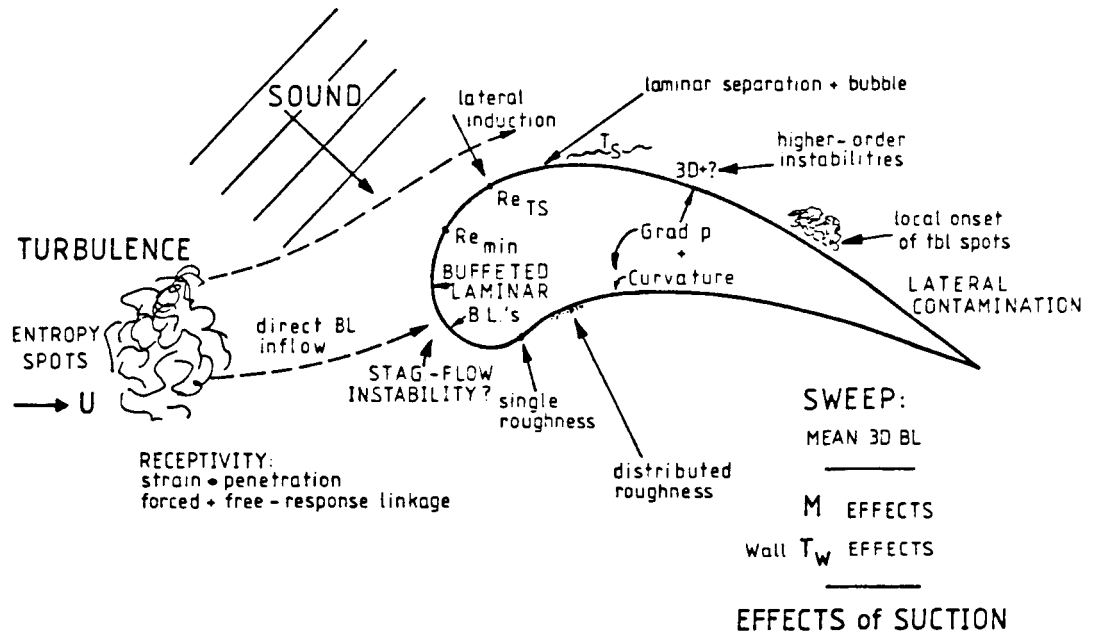


Fig. 1a - Typical transition issues in external flows

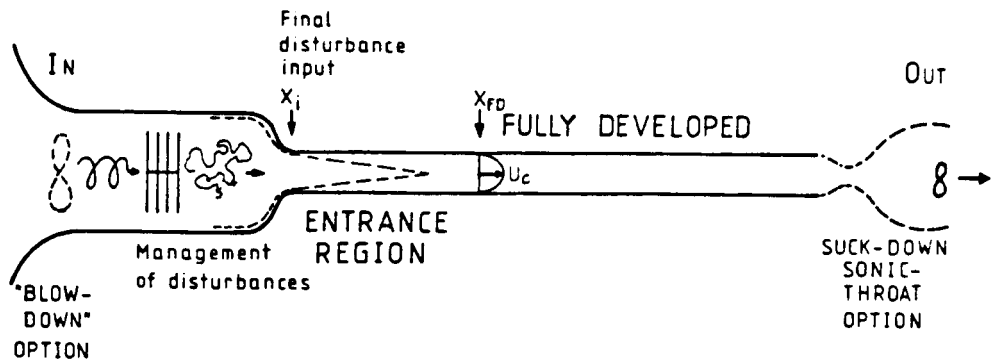


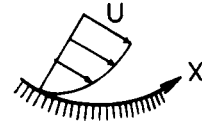
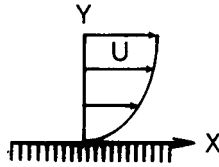
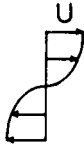
Fig. 1b Internal flow facility

# INSTABILITIES → TURBULENCE

Dynamics & Kinematics of VORTICITY DISTRIBUTIONS  
(BIOT-SAVART IMAGERY)

$$\underline{\omega}(x,y,z,t) = i\underline{\xi} + j\underline{\eta} + k\underline{\zeta}$$

SHEAR LAYERS

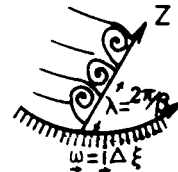
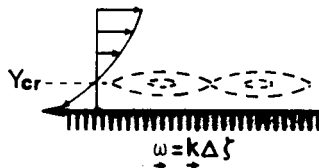
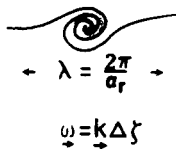


initially quasi-homogeneous in x and z.

SEQUENCES OF some simultaneous } INSTABILITIES } 1,2,3... TURBULENT STRUCTURES ...  
 $\underline{\omega}$  RESTRUCTURING

First Primary Instability ≡ Dehomogenization ~ Restructuring

MECHANISM: inflectional in x viscosity conditioned tuned in z centrifugal



**FIRST:** NET VORTICITY CHANGES AVERAGE TO ZERO  $\sum \Delta \omega = 0$

Initially linearizable :  $\cos a_r(x-c_r t)e^{-a_r c_r t}$      $\cos a_r(x-ct)e^{-a_r x}$      $\cos \beta z e^{-a_r x}$

followed by slower nonlinear growth

possible approach to "saturation"  $\approx$  "neutral" max. of first restructuring

USUAL ASSUMPTION (not sufficiently general)

secondary Instability from local nonlinear equilibrium  
initially linearizable around this

linear D.E. with periodic coefficients

FLOQUET SYSTEMS ≡ PARAMETRIC INSTABILITIES

FIG. 2 VORTICITY RESTRUCTURING IN INSTABILITIES

**Examples**

**SECONDARY** : pairing in mixing layers ( multiple amalgamation when stimulated by  $f/n$  )  
 tilt & stretching in C,H&K breakdowns in BL's  
 rotating wavy Taylor cells in Couette  $\Omega_1$  flow

**TERTIARY** : hairpin-vortex formation (3D inflectional) in K breakdown  
 2-frequency wavy Taylor cells

↓  
 ULTIMATELY OPERATIONALLY INDISTINGUISHABLE FROM  
**TURBULENT STATES** characterised by 4 key **SYNDROMES**

- ① irregularity (disorder,partial) → stochastic nonlinear systems
- ② 3 Dim vorticity (eddying) → ensemble of loosely coupled deformable gyroscopes
- ③ diffusion far in excess of molecuxar mixing → both friend and foe  
 ↘ on a large range of scales  
 ∴ broad-band spectra
- ④ dissipation

see-Tennekes & Lumley (1972)

and film by R. W. Stewart (1968) and 8-page summary

**RESTRUCTURING CONTINUES** in turbulent shear flows  
 --> large - scale coherent structures, fine-scale intermittency.

( ① represents strange behavior in continuum mechanics -  
 -apparently common in **NONLINEAR DISSIPATIVE SYSTEMS** with  
 "strange attractors" larger number of degrees of freedom )

**EXISTENCE of  $Re_{mint}$  for self sustaining wall turbulence**

on scales corresponding to the thickness  $\delta$  of the layer

upstream of  $Re_{mint}$   
 buffeted lam. BL's  
 lacking true turbulent  
 transport ③

presumably through intermittent "BURSTS"  
 of the viscous sublayer, correlated disturbance

motions producing  
 negative Reynolds  
 stresses - $\rho u'v'$

SWEEP

EJECTION

$v^-$   
 $u^+$

$v^+$  (large)  
 $u^-$



mushrooms or  
 like hairpin loops ?

**IN HIGLY ACCELERATED TBL BL's**

the viscous sublayer is stabilized, bursts stop.  
 the sublayer becomes a "buffeted lam. BL", decoupled from the  
 wake-like, decaying turbulent outer layer (STERNBERG 1954).

This is one mode of **RELAMINARIZATION**.

see NARASIMHA & SREENIVASAN (1979) for other modes.

**FIG.3 HIGHER RESTRUCTURING AND TURBULENCE**

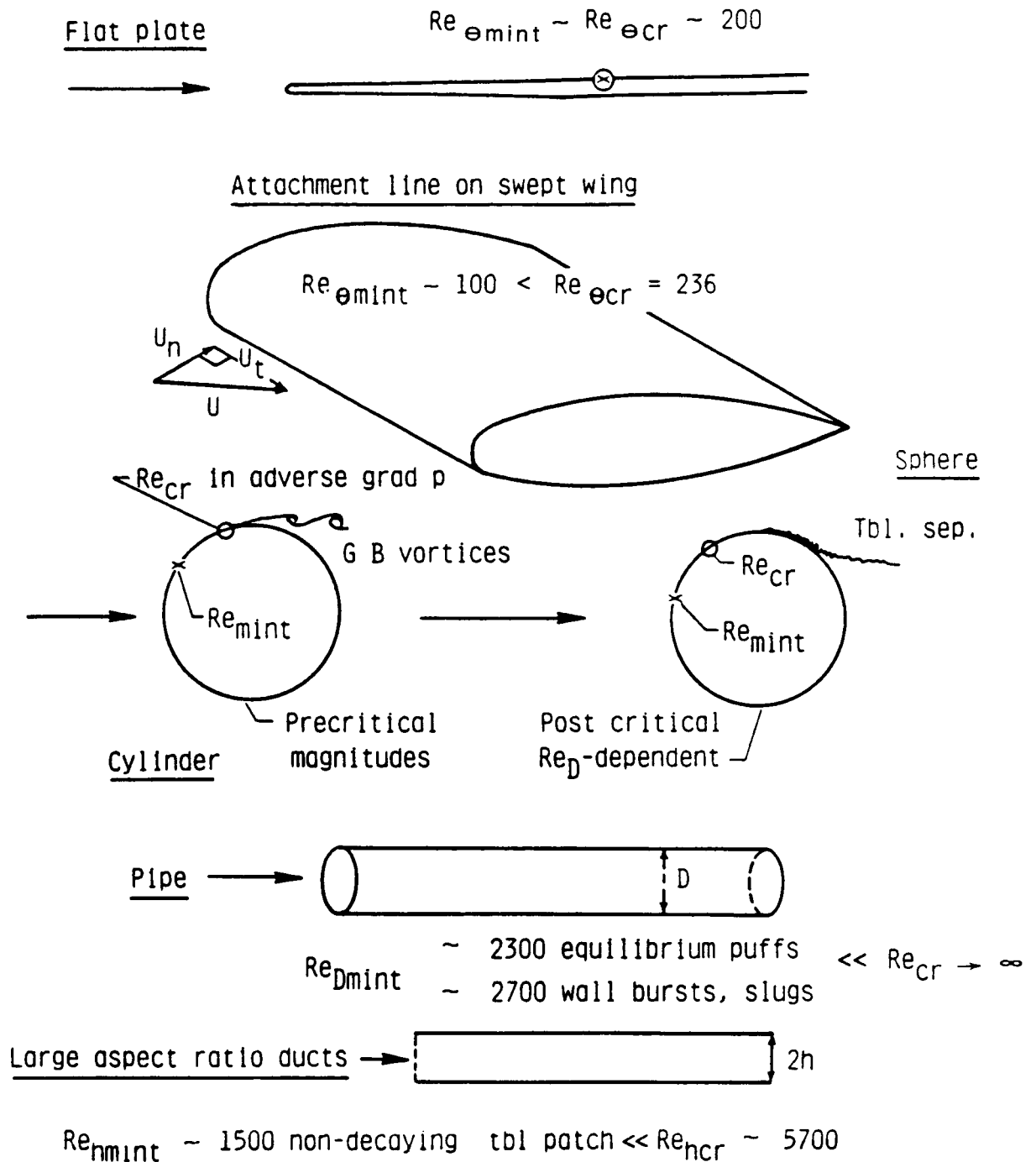
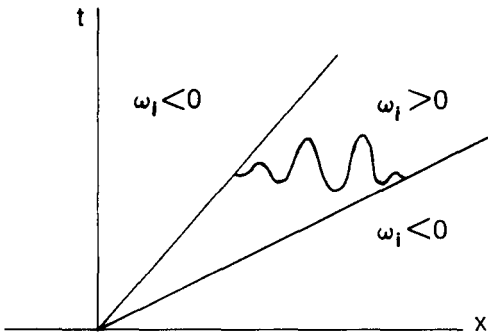


Fig.4 : Minimum  $Re$  for self-sustained turbulence compared to linear critical  $Re$  for T-S like instabilities.

**LINEARIZED RESPONSE to LOCAL IMPULSE DISTURBANCE at  $x=0, t=0$**

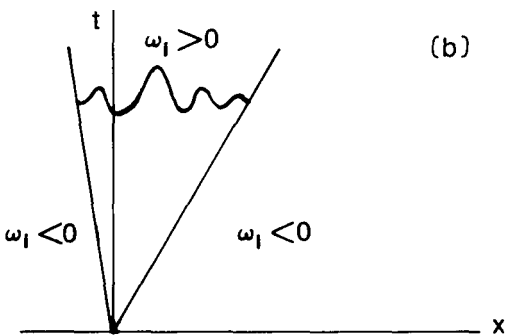
proportional to  $e^{i(kx-\omega t)}$



(a)

**CONVECTIVE INSTABILITY**

e.g. Boundary Layers  
**GASTER SPOTS (1975)**



(b)

**ABSOLUTE INSTABILITY**

Onset Criterion:  
group velocity  
 $c_g = \partial\omega / \partial k = 0$   
(double root)

**STABILITY**

$\omega_i < 0$  for all  $x, t$ :  
impulse response decays everywhere

See **HUERRE + MONKEWITZ (1985) JFM 159,151**

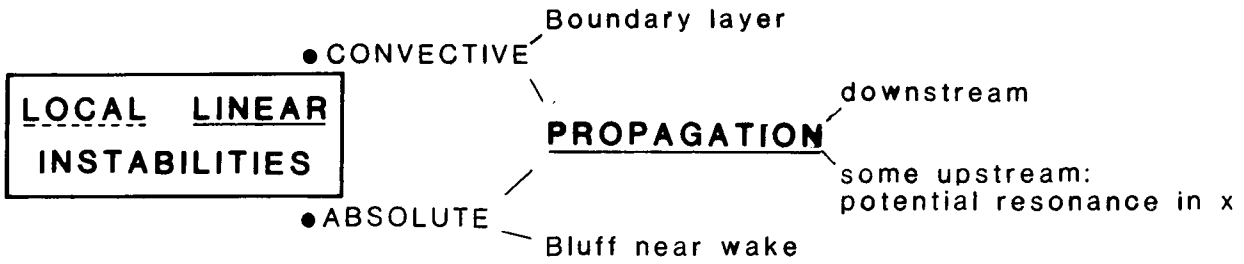
**TEMPORAL** → linear response to continuous  $A \sin x$  at  $t=0$

**INSTABILITY** → dependent on INITIAL CONDITIONS in  $x$  and/or  $t$

**SPATIAL** → linear response to continuous  $A \sin \omega t$  at  $x=0$

**FIGURE 5**

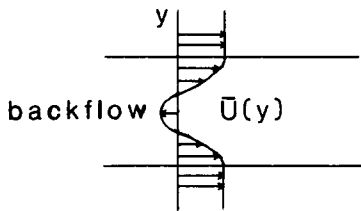




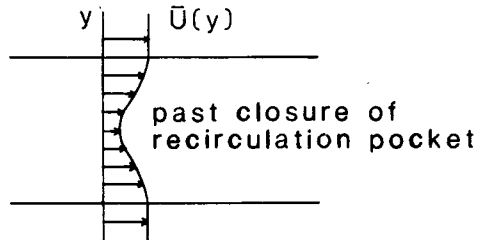
LOCAL means:

at each  $x$ , replace  $x$ -varying shear layer by parallel, constant layer with local mean profile  $\bar{U}(y)$  - neglects strong destabilizing adverse pressure gradient near body!

for Bluff wake



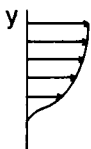
Near: absolutely unstable



Farther: convectively unstable

**RIGOR** in usage of local mean profile of vigorously oscillating wake?

**PROBLEM** of **NONLINEAR UPSTREAM EFFECTS** through **PRESSURE**:



This unsteady feedback converts the linearly convectively unstable mixing layer into a weakly (non-robust) absolutely unstable one!

**GLOBAL INSTABILITY** arises from 'resonance' in  $x$  when non-parallel  $x$  evolution is directly taken into account.

Modeling via Ginsburg-Landau equation, CHOMAZ, HUERRE REDEKOPP (1988, Phys.Rev.Letters, 60,25) show:

**NEED** long enough  $x$  range of Absolute Local Instability to build up an unstable eigenfunction in  $x$  on top of the local  $y$  eigenfunction of the layer.

**PROBLEM** of Boundary Conditions in  $x$ , especially at body

**GROWTH TO NONLINEAR SATURATION and ENERGY BALANCE**

**SYSTEM** then **ROBUST** to environmental disturbances!

**HYDROACOUSTIC GLOBALLY UNSTABLE SYSTEMS**

e.g. jet edge-tone:

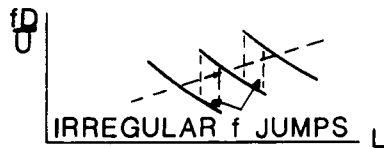
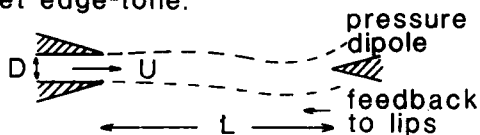


**FIG.6** CONVECTIVE, ABSOLUTE and GLOBAL INSTABILITIES

# MIXING LAYER INTERACTIONS

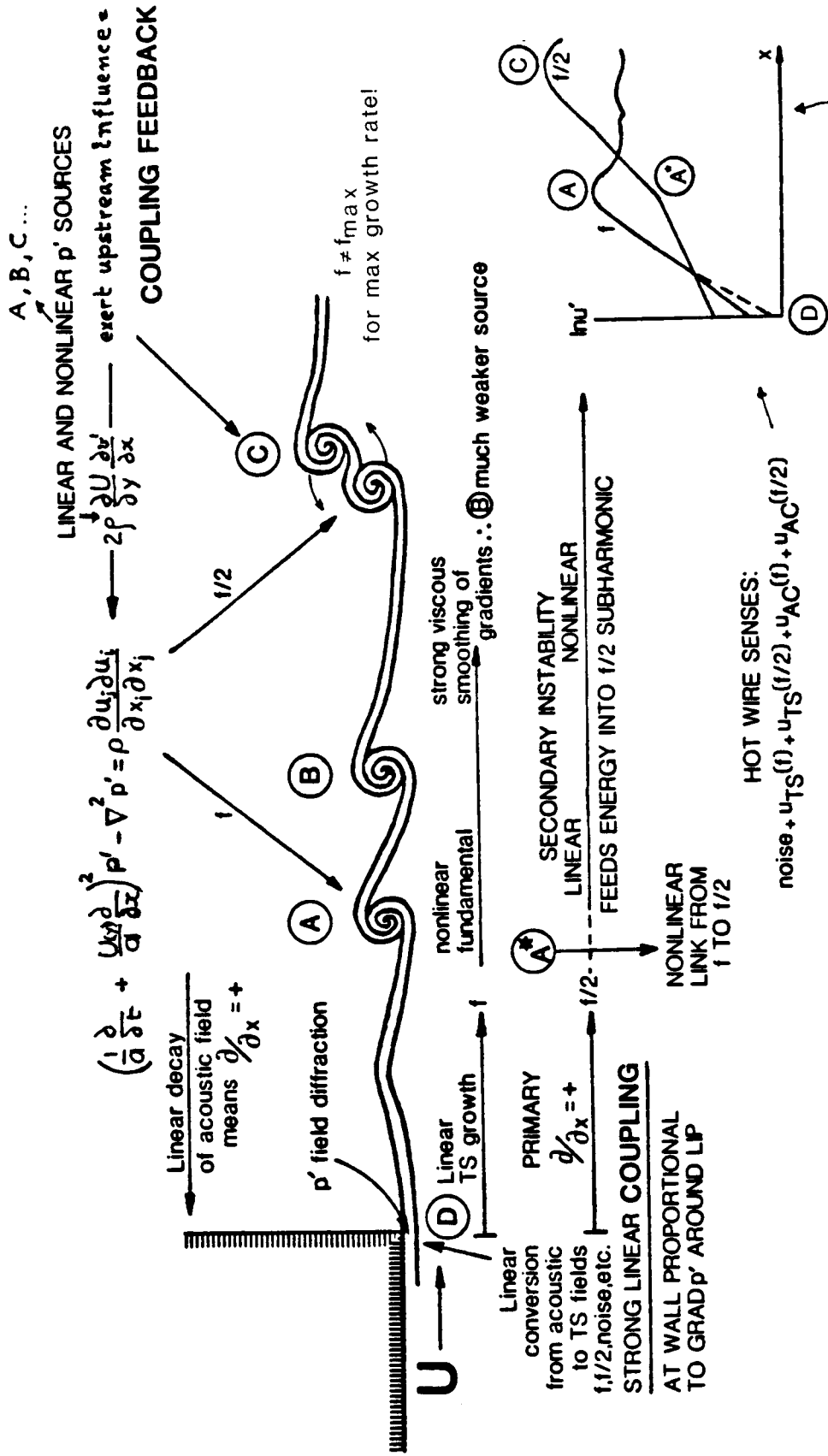
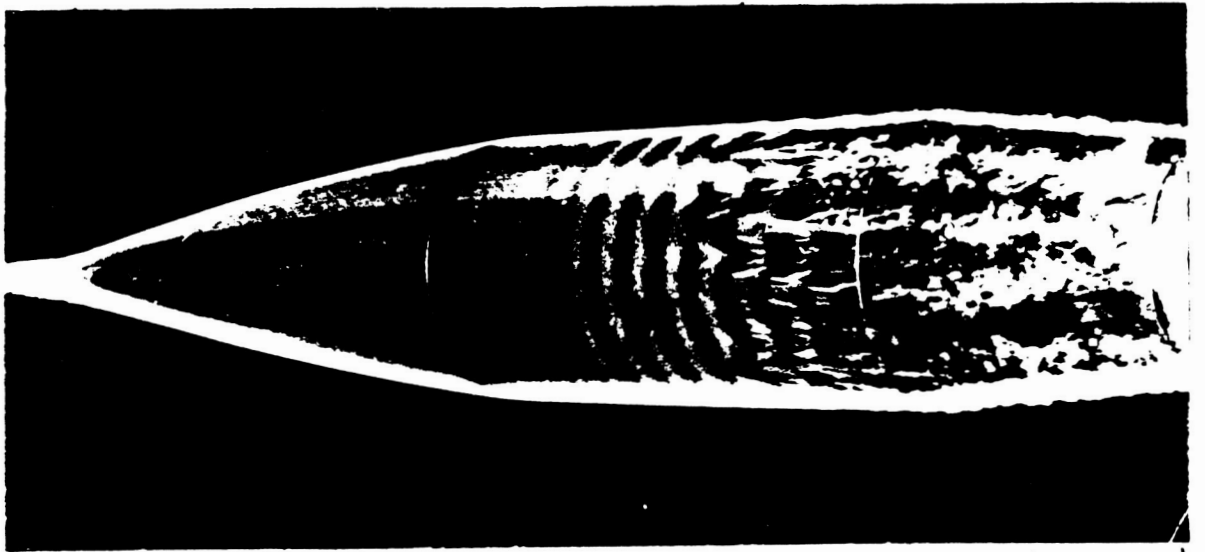
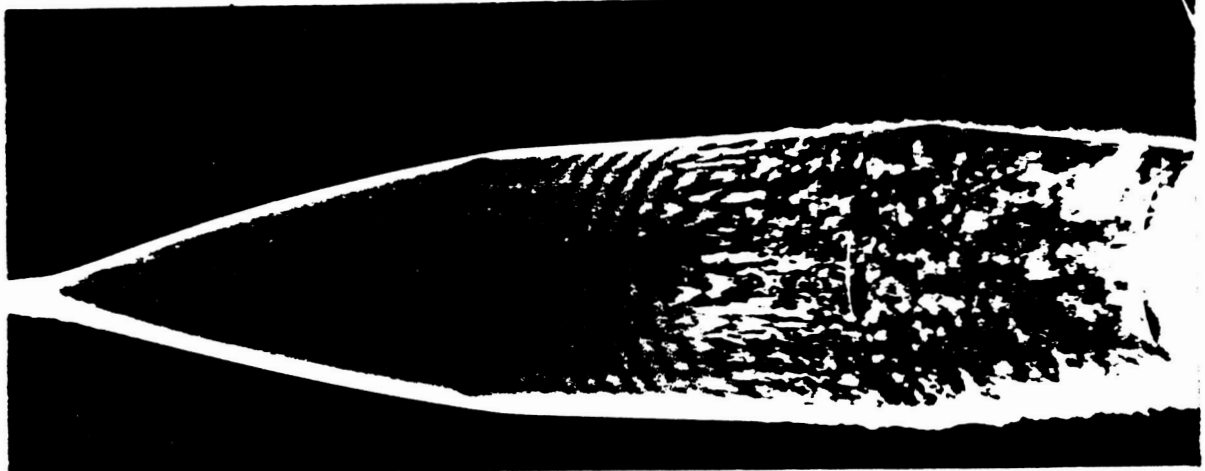


FIGURE 7 Summary of primary and secondary instabilities and their upstream influence on artificially unstimulated disturbances at origin of the layer; conditions correspond to the inset, courtesy of Drubka (1982). Locking of subharmonic  $f/2$  onto the nonlinear fundamental  $f$  at  $A^*$  initiates the secondary instability. TS designates unstable modes of the primary instability.



$Re_L = 814,000, \alpha = 0$

excitation at  $f = 551 \text{ Hz}$   $\uparrow$   $785 \text{ Hz}$   $\downarrow$



Kegelman and Mueller (1984), AIAA Jour.

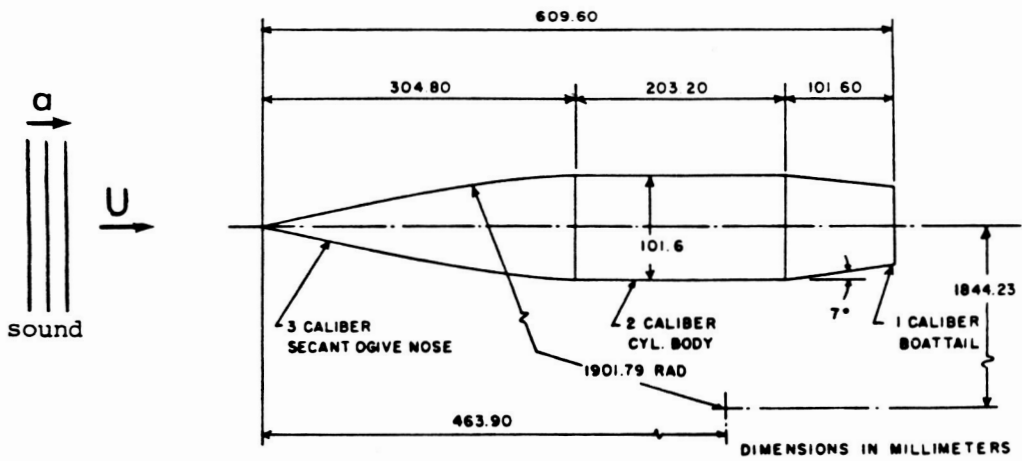
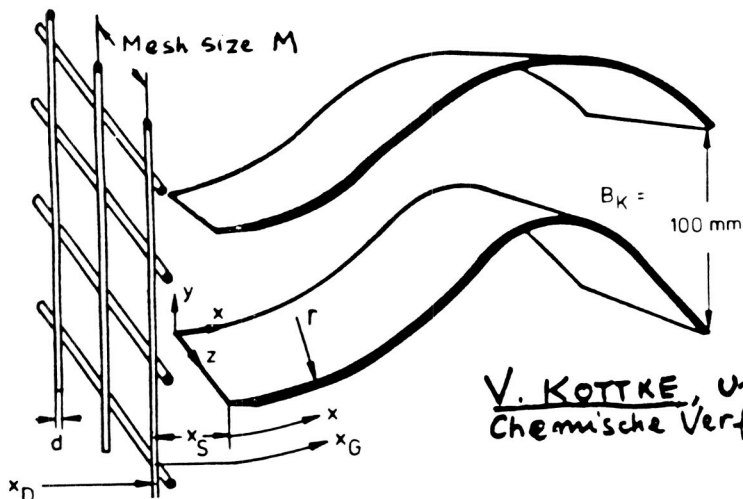
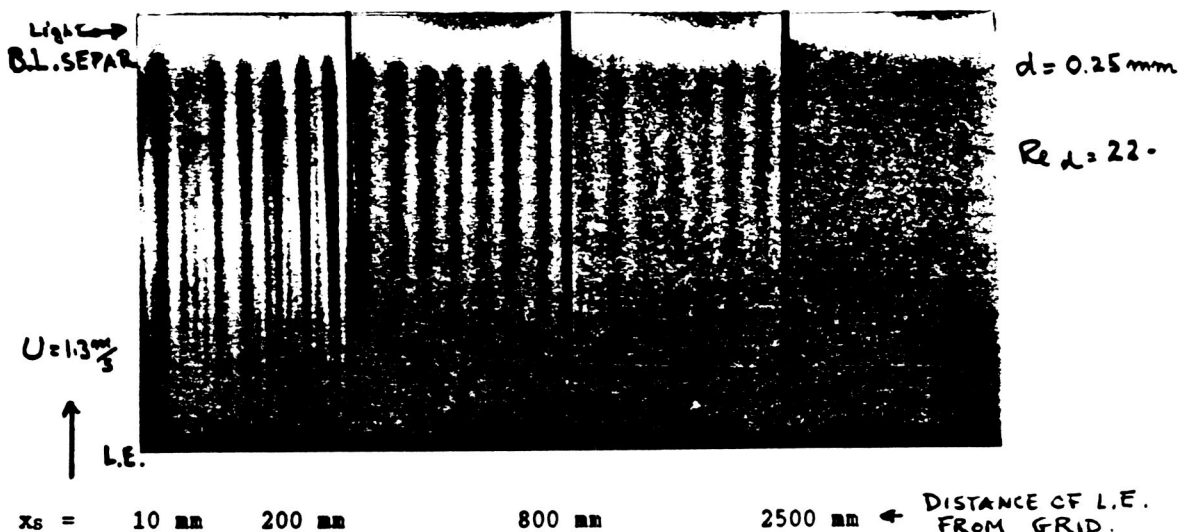


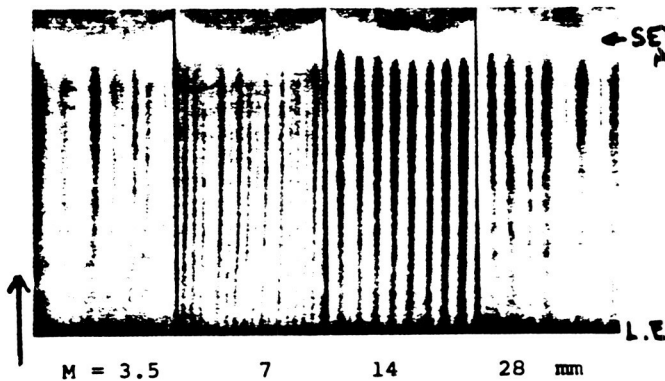
Figure 8 Sound induced TS waves on ogive-cylinder body at U of 21.6 m/s



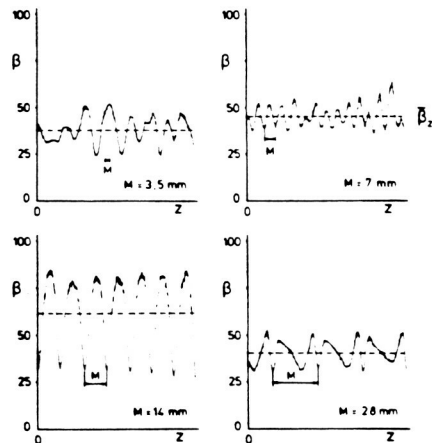
V. KOTTKE, Univ. Stuttgart  
Chemische Verfahrenstechnik



Local mass transfer as color density distribution



Mass transfer distribution for different mesh sizes,  $M$ .  
( $x_S = 100$  mm,  $U = 1.3$  m/s)



Local mass transfer coeff  $\beta$   
( $x = 150$  mm)

FIG. 9 EFFECT OF GRIDS ON GOERTLER INSTABILITY

## DISTURBED ENVIRONMENT in OPEN-FLOW SYSTEMS

### PROBLEM of DIAGNOSTICS of ONCOMING FIELDS and IMPURITIES

SPECTRA! minimum of 2 INSTRUMENTS to separate free-stream Tu and p' fields

STRAINING of DISTURBANCE FIELDS (as they approach the body and shear layer) is part of the problem, especially near stagnation regions, sharp edges, upstream contraction, also by the shear in the boundary layer itself.

#### ● IRROTATIONAL UNSTEADY PRESSURE FIELDS $p'(x,y,z,t)$

- (a) isentropic  $p', \rho', T'$ : Acoustic HYPERBOLIC behavior especially at higher f: propagating wind-tunnel modes, resonances.
- (b) constant-p (near-field sound~pseudosound): ELLIPTIC at lower f. Wind Tunnels: SEPARATION in DIFFUSORS, Helmholtz instabilities.

#### ○ WALL VIBRATIONS: receptivity similar to p' fields.

#### ● VECTOR VORTICITY FIELDS, $\omega'$ , True TURBULENCE

- (a) QUASI-STEADY STREAMWISE  $\omega'_x$ : essentially PARABOLIC, due to upstream bends, guide vanes, screens etc. Important sources: LEADING-EDGE IMPERFECTIONS, SURFACE ROUGHNESS.

- (b) UNSTEADY  $\omega'_x, \omega'_y, \omega'_z$  with associated  $\gamma'$  field, PARABOLIC: Larger-scale free-stream Tu structures  $\rightarrow$  intermittency in x, t; the sharp x, t dependence for each structure may induce TS wave packets across streamlines or when penetrating shear layer? Tu amplitude decay in x important, but much slower.  $\omega$  modes are forceable by vibrating ribbon, pressure holes, inhomogeneous time-dependent wall suction and heating.

#### ● ENTROPY FIELDS $\sigma'$ (Temperature-density fluctuations at constant p)

- Arise in any heat addition, (if explosive  $\rightarrow$  transient p' field is added); propagate essentially PARABOLICALLY along main stream lines. Do induce unstable vorticity modes especially at higher Mach numbers.

#### ● PARTICULATES and AEROSOLS

- Are known to expedite transition to turbulence, but how? Presumably by generating local, traveling vorticity fields near walls.

#### ○ EACH DISTURBANCE FIELD may have distinct MULTIPLE linear and nonlinear RECEPTIVITY PATHS $\rightarrow$ COMPETITION within and among the DISTURBANCE FIELDS

which is most dangerous for a given configuration?

FIGURE 10

# INSTABILITIES AND ROAD TO TURBULENCE in OPEN-FLOW SYSTEMS

ARE FORCED by ENVIRONMENTAL DISTURBANCES  
(except in rare cases of global-absolute instabilities)

RECEPTIVITY: conversion of external disturbances into  
internal homogeneous growing vorticity modes

## SMALL DISTURBANCES

Linearizable Receptivities:  
● in principle, SOLUTIONS to

### NONHOMOGENEOUS



PARTICULAR (FORCED) SOLUTION

**PLUS**

all HOMOGENEOUS SOLUTIONS  
needed to satisfy together all  
**BOUNDARY CONDITIONS** in space  
and time, EXACTLY (not on the  
average, in case of turbulent  
disturbances) These conditions fix  
the coeff  $C_n$  in the symbolic form:

$$\text{Sol}_{\text{part}} + \sum_n C_n \cdot \text{HomoSol}_n$$

For larger  $x$  and  $t$  all but one  
(or few:  $j$ )  $\text{HomoSol}_n$  and  $\text{Sol}_{\text{part}}$   
decay, leaving the dominant  
response  $C_j \cdot \text{HomoSol}_j$

Ex: BECHERT (1988) JFM 186,47

## LARGE DISTURBANCES

Concept of **NONLINEAR  $Re_{\text{mint}}$**   
for self-sustenance of turbulence  
in a given Boundary Layer,  
generally below linear  $Re_{\text{cr}}$

### UNKNOWN NEW $x, y, z, t$ - dependent BASE FLOWS

If locally linearizable:  
**RAPID INFLECTIONAL INSTABILITIES**  
(with forcing)



### **BYPASSES**

of previously explored linearized  
fields and mechanisms.

#### EXAMPLES

- Large, single-PROTUBERANCE  
instability and transition
- Impingement of wakes from  
upstream in turbomachinery
- Turbulent patches in 2D  
Poiseuille ducts
- Larger distributed ROUGHNESS

see Morkovin(1984) 'Bypass  
Transition', NASA CP-2386,  
Sympo: Transition in Turbines  
NASA Lewis Res.center

---

**HYBRID CASE:** Enhanced TS and Herbert receptivities to free-stream fields  
due to mean-flow changes **BELOW** the heights of smaller distributed roughness,  
CORKE, BAR-SEVER, MORKOVIN(1986) Phys. Fluids 29,3199

FIG. 11 ENVIRONMENTAL FORCING & RECEPTIVITY



ORIGINAL PAGE IS  
OF POOR QUALITY

$f_1$  locked on  
natural-street  
frequency  $f_n$   
= 4.075 Hz



quasi-periodic  
response to  
off-street  $f_1$  :  
 $f_1 = 3.5$  Hz  
 $f_2 = 4.9$  Hz



chaotic laminar  
 $f_1 = 3.55$  Hz  
 $f_2 = 4.075 = f_n$   
 $f_3 = 5.42$  Hz  
some 3D motion



no forcing ;  
turbulence tripped  
symmetrically  
by wires in B.L.  
U = 13 cm/sec

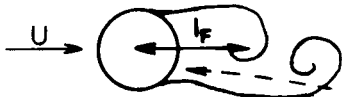


COURTESY: K. Stuber and M. Gharib

FIG. 12 EXCITED STATES IN SLENDER WAKE

**SOME ROADS to TURBULENCE ? CHAOS**

- Q: can shear layers growing in x have STEADY strange attractors?
- Q: can chaos theory accomodate lam.-Tu coexistence?



$45 < Re < 160$

$Re > 200$   
 Tu downstream  
 ↓  
 marches upstream

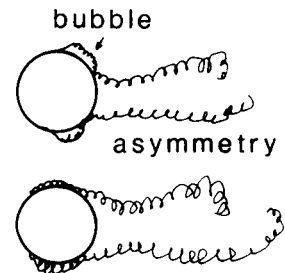
**GLOBALLY** unstable system **NEAR BODY**  
 some local feedback through unsteady backflow;  
 stable, LOCKED "clockwork" oscillator  
 3D-instab.(absolute?); role of  $\omega_x$  disturbances?  
 sym.-antisym. mode competition? Gerrard(1978)  
 Drop in  $C_L$ , rise in  $p_B$  and  $l_F$ -unexplained  
 Reversed for  $Re > 2000 \sim 10,000$ , why?

Tu reaches fluid in first shedding vortex

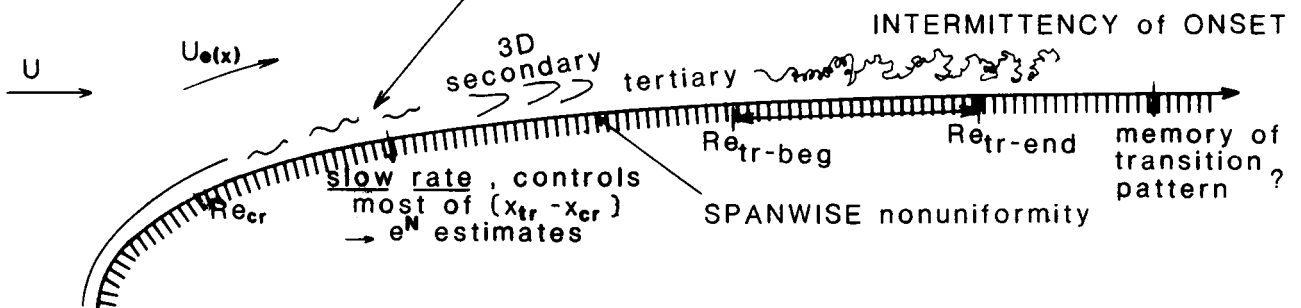
Tu in separating layer causes reattachment and bubble;  $Re \sim 2 \cdot 10^5$   
**IMPORTANT SPANWISE NONUNIFORMITY**

Tu onset upstream of lam.sep., crooked tbl.sep. line, low  $C_L$ ;  $Re \sim 1.5 \cdot 10^6$

Tu marches upstream in thin B.L.; roughness sensitive; wake widens, mild  $C_L$  rise as sep. line straightens



**B.L.:** **CONVECTIVELY** unstable **RESPONSE** to low free-stream Tu:  
 superposition of lam. TS spots, amplifying quasi2D in x



As  $U$  increases, pattern moves upstream, but  $Re_{tr}$  not constant! Unit-Re effects!

**UNLIKE** for pure STRANGE ATTRACTORS, **SIGNAL IRREGULARITY** strongly **NOISE DEPENDENT**

- Q: Any way of experimentally sensing the intrinsic SA irregularity if present?
- Q: Invariance of such intrinsic measures in y and z, and especially in x?

**FIG. 13 EVOLUTION TO TURBULENCE IN GLOBALLY AND CONVECTIVELY UNSTABLE EXAMPLES**



**CLOSED-FLOW SYSTEMS**

credited with "yes, but" verifications of theory by Guckenheimer (1986)  
 (a) **RECYCLING** of same interacting eddies of constant size  
**AN ITERATIVE FEATURE**  
 basic to theory of chaos

Measurements made at single point  
 (with exception of Heslot, Castaing, Libchaber, (1987))

**ASSUMPTIONS**

- (1) There exists a unique strange attractor, S.A., for a given set of system parameters.
  - (2) Time trace at single point characterizes qualitative properties of the **WHOLE SYSTEM**, including S.A.  
 (How widely is this quality-invariance in x,y,z demonstrated?)
  - (3) Initial and continued external noise does not modify intrinsic S.A. structure (despite the fact that harmonic forcing adds a new phase dimension)
- Q<sub>0</sub>: Procedures for separating intrinsic chaotic features from extrinsically driven random features of the response?

**OPEN-FLOW SYSTEMS**

controversial: what is really measured in an x-dependent development?  
 (b) Vorticity fields passing by with very limited filtered upstream influence  
 (c) Vorticity structures growing in thickness in x - stability changing in x!

Experiments adopted single-point techniques without modification in processing to account for (b) and (c)

- (1) there may not be an asymptotic S.A. assignable to any "local thickness" at x - could S.A. be a local property?
- (2) Onset of Tu is local in x,z,t, with spatially limited range of influence.  
 {Laminar-Tu interfaces } convected past groupings of large eddies } any single probe - traces can hardly characterize whole system.
- (3) Open-flow systems (with exception of short segments of bluff wakes and variable density jets) are all convectively unstable. Receptivity and instabilities yield **AMPLIFIED**, mildly-filtered **NOISE-CONDITIONED STRUCTURES** up to order  $\delta(x)$ , with slower-longer scale extrinsic modulations.

- Q<sub>1</sub>: To what extent have open-flow probes extracted fictitious measures, not corresponding to any S.A.?
- Q<sub>2</sub>: Can procedures operating on space-time traces, e.g.  $u(x,t)u(x+\Delta x, t+\Delta x/U_c)=f(t)$  extract better intrinsic characterization of x-t evolving groups of large eddies?
- Q<sub>3</sub>: What does one do with such characterizations, say of convective S.A., if successful?  
 Establish a dictionary of strange attractors as related to physical flows?

FIG. 14 SOME EXPERIMENTAL ISSUES

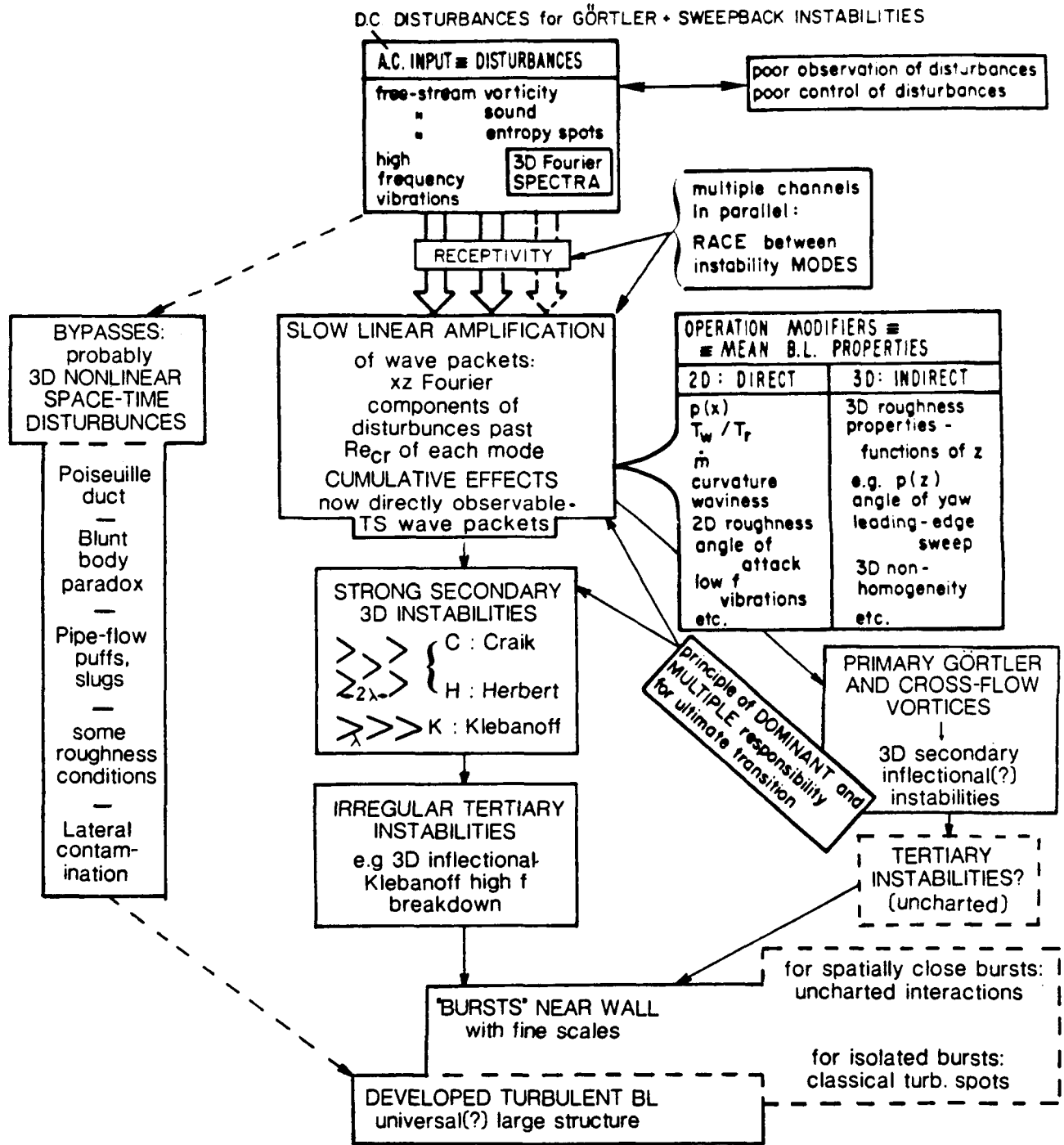
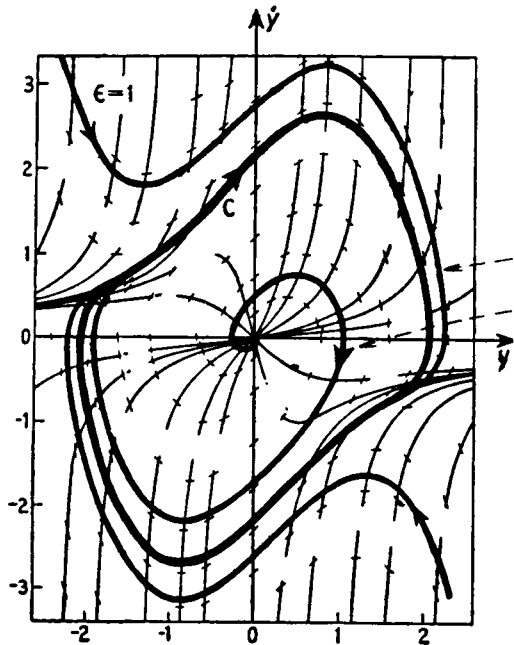


FIGURE 15. 1984 system portrait of environmentally stimulated vorticity perturbations on their evolutionary paths to turbulence in undistorted boundary layers and ducts.

GENERAL PRINCIPLES OF POOR QUALITY

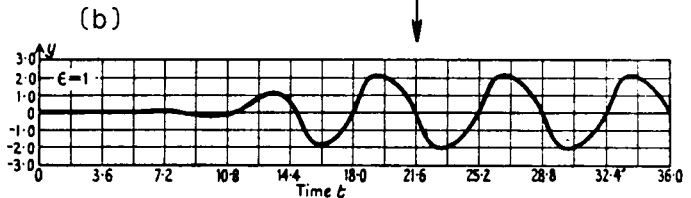
**Forced Van der Pol oscillator:**  
 $\ddot{y} + \epsilon(y^2 - 1)\dot{y} + y = b\epsilon\omega\cos\omega t$

(1) unforced case  $b=0$   
 autonomous system



(a) } OUTER } TRAJECTORIES in phase space  
 } INNER } both attracted to the same  
 set of points: **LIMIT CYCLE C** ;

therefore motion becomes  
 periodic in time, has  
**TIME RECORD**



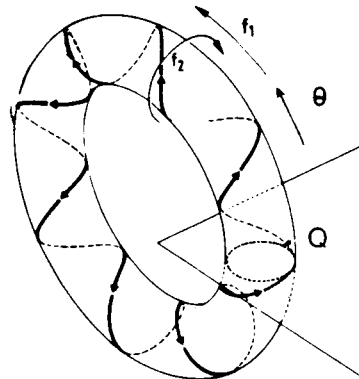
(2) forced case  $b \neq 0$

To make system autonomous (free of explicit  $t$ -dependence) introduce a third dimension (phase variable)  $\theta$  by setting  $\dot{\theta} = \omega$ . Equivalent system of three first-order equations is:

$$\dot{y} = \epsilon \{ x - (y^3/3 - y) + b \sin \theta \} ; \quad \dot{x} = -y/\epsilon ; \quad \dot{\theta} = \omega : \text{PARAMETERS } \epsilon, b, \omega$$

Solutions trajectories attracted to:  
 curves on a limiting **TOROIDAL SURFACE** →  
**STRANGE ATTRACTORS**: collection of infinite sets of convoluted 'parallel' surfaces with spacing locally approaching infinitesimal, studied by Poincare' sections, P →

PROPERTIES have aperiodic, bounded traces in time, corresponding to broad-band spectra  
 Positive Lyapunov exponents trajectory divergence  
Supersensitivity to initial conditions in phase space



After Mc Lachlan (1947), Oxford Un. Press and Berge' Pomeau and Vidal (1986), John Wiley & Sons

(c)

**FIG. A-1 ROAD TO CHAOS IN A FORCED NONLINEAR OSCILLATOR**



# Report Documentation Page

1. Report No. NASA CR-181693 ICASE Report No. 88-44		2. Government Accession No.		3. Recipient's Catalog No.	
4. Title and Subtitle RECENT INSIGHTS INTO INSTABILITY AND TRANSITION TO TURBULENCE IN OPEN-FLOW SYSTEMS				5. Report Date August 1988	
				6. Performing Organization Code	
7. Author(s) Mark V. Morkovin				8. Performing Organization Report No. 88-44	
				10. Work Unit No. 505-90-21-01	
9. Performing Organization Name and Address Institute for Computer Applications in Science and Engineering Mail Stop 132C, NASA Langley Research Center Hampton, VA 23665-5225				11. Contract or Grant No. NAS1-18107, NAS1-18605	
				13. Type of Report and Period Covered Contractor Report	
12. Sponsoring Agency Name and Address National Aeronautics and Space Administration Langley Research Center Hampton, VA 23665-5225				14. Sponsoring Agency Code	
15. Supplementary Notes Langley Technical Monitor: Richard W. Barnwell Submitted to Proc. 1st National Congress on Fluid Dynamics Final Report					
16. Abstract Roads to turbulence in open-flow shear layers are interpreted as sequences of often competing instabilities. These correspond to primary and higher-order restructurings of vorticity distributions which culminate in convected spatial disorder (with some spatial coherence on the scale of the shear layer) traditionally called turbulence. Attempts are made to interpret these phenomena in terms of concepts of convective and global instabilities on one hand, and of chaos and strange attractors on the other. The first is fruitful, and together with a review of mechanisms of receptivity provides a unifying approach to understanding and estimating transition to turbulence. In contrast, current evidence indicates that concepts of chaos are unlikely to help in predicting transition in open-flow systems. Furthermore, a distinction should apparently be made between temporal chaos and the convected spatial disorder of turbulence past Reynolds numbers where boundary layers and separated shear layers are formed.					
17. Key Words (Suggested by Author(s)) transition in shear flows, convective instability, receptivity, chaos			18. Distribution Statement 34 - Fluid Mechanics and Heat Transfer 64 - Numerical Analysis Unclassified - unlimited		
19. Security Classif. (of this report) Unclassified		20. Security Classif. (of this page) Unclassified		21. No. of pages 83	22. Price A05